Mixed Tiling Systems

Alexandra Grant

May 2018

A thesis submitted for the degree of Bachelor of Philosophy (Honours)
of the Australian National University

Declaration

The work in this thesis is my own except where otherwise stated.

Alexandra Grant

Acknowledgements

First and foremost, I would like to thank my terrific supervisor Michael Barnsely. Thank you for giving me a taste of mathematical research and encouraging me to think independently!

I would also like to thank the many fantastic academics and lectures in the MSI whose great courses have taught me lots of interesting maths. Thanks to my fellow honours students in both the 2017 and 2018 cohorts for creating a fun and supportive study environment.

I thank my housemates and friends for keeping life full of adventures. I am also grateful for the many spectacular running trails around Canberra. Finally, I would like to thank my parents and brother for their love and support over the years.

Abstract

This thesis extends the theory of tiling iterated function systems developed in [BV18] and connects the theory to other areas of the tiling literature. The first two chapters provide background material, introduce tiling iterated function systems, and discuss properties of the tilings generated from these systems. Simple examples are showcased and repeatedly referenced throughout the thesis. The third chapter links the symbolic tiling theory to Anderson and Putnam tiling theory [AP98] and the fourth chapter connects the theory to the work of Bandt on neighbour graphs [BM18]. An extension to the neighbour graph theory is proposed which allows the application of these techniques to a wider range of tiling iterated function systems. The final and title chapter of this thesis extends the symbolic tiling theory to mixed tiling systems. The notation and general framework for creating tilings from a family of tiling iterated function systems is presented. The examples considered in the mixed setting cover one-dimensional tilings, tilings with statistical circular symmetry, and tilings made from tiles with no interior. It is explained how these ideas are related to V-variable and superfractal theory.

Contents

Chapter 1

Tiling Iterated Function Systems

This chapter introduces the algebraic and symbolic tiling theory developed in research by Barnsley and Vince (B & V) [BV17b, BV18]. Using the inverse maps of an iterated function systems to study tilings is well-established in the literature (see [Ban97] for example). A main contribution of B & V is presenting a simple, unifying method to construct tilings from iterated function systems that fully captures the symbolic story and easily applies to tilings of fractal blow-ups where the tiles may have no interior.

We begin, in section 1.1, by defining graph iterated function systems and introducing convenient notation. Section 1.2 reviews basic fractal theory on attractors and code space. These two sections prepare the reader for section 1.3 which defines and discusses tiling iterated function systems. Finally, section 1.4 showcases two key examples.

The notation, definitions and theorems in this chapter mostly follow [BV18]. The other chapters of this thesis use the language introduced here and build on this symbolic framework. In particular, chapter 2 focuses on tiling iterated function systems that satisfy a property known as 'local rigidity'.

1.1 Graph Iterated Function Systems

A hyperbolic iterated function system (IFS) consists of a complete metric space together with a finite set of strictly contractive maps. Since all the IFSs we consider are hyperbolic, we refer to them simply as IFSs for the remainder of this thesis. It is well-known that these systems can be used to create self-similar fractals (see [Hut81] for example). Also known, but maybe less widely appreciated, is that 'quasiperiodic' (defined in section 1.3) tilings can be constructed as fractal blow-ups of certain IFSs. We concern ourselves with the generalisation of these ideas to the graph (directed) IFS setting [BV18].

Definition 1.1. Let $\mathcal{F} = \{f_1, f_2, ...f_N\}$ be a finite set of invertible contraction maps $f_i : \mathbb{R}^M \to \mathbb{R}^M$ with contraction factors $0 < \lambda_i < 1$ for $i \in \{1, ...N\}$. Let $\mathcal{G} = (\mathcal{E}, \mathcal{V})$ be a finite strongly connected directed graph with edges

$$\mathcal{E} = \{e_1, e_2, ...e_{|\mathcal{E}|}\} \text{ with } E = |\mathcal{E}| = N$$

and vertices $\mathcal{V} = \{v_1, ...v_{|\mathcal{V}|}\}$ with $V = |\mathcal{V}| \leq N$. The graph $\mathcal{G}$ provides the order in which the functions $\mathcal{F}$ may be composed from left to right. We call $(\mathcal{F}, \mathcal{G})$ a graph IFS. In general, we denote the edges in $\mathcal{G}$ by the indices $\{1, 2, \ldots N\}$ and the vertices by elements of the set $\{1, 2, \ldots V\}$.

The graph $\mathcal{G}$ being strongly connected means there is a directed path from any vertex of the graph to any other vertex. We introduce a supply of convenient notation for various sets of vertices and edges in $\mathcal{G}$.

Notation 1.2. Define

- $\mathcal{E}_{v,w}$ as the set of directed edges in $\mathcal{G}$ from vertex w to vertex v,
- $\mathcal{E}_{v,*} := \{u \in \mathcal{E}_{v,w} : w \in \mathcal{V}\}$ as the set of directed edges with the final vertex specified,
- $\mathcal{E}_{*,v} := \{u \in \mathcal{E}_{w,v} : w \in \mathcal{V}\}$ as the set of directed edges with the initial vertex specified,
- Σ_0 as the empty string $\emptyset$,
- Σ_k as the set of directed paths in $\mathcal{G}$ of length $k \in \mathbb{N}$,
- $\Sigma_* := \cup_{k \in \mathbb{N}_0} \Sigma_k$ as the set of directed paths of finite length,
- Σ_∞ as the set of directed paths of infinite length, and
- $\Sigma := \Sigma_* \cup \Sigma_\infty$.

So Σ is the set of finite and infinite paths in $\mathcal{G}$ that by Definition 1.1 corresponds to the allowed compositions of functions from $\mathcal{F}$. The sequence of directed edges $(e_{\sigma_1}, e_{\sigma_2}, \ldots e_{\sigma_k})$ corresponds with the composition $f_{\sigma_1} \circ f_{\sigma_2} \circ \ldots \circ f_{\sigma_k}$.

We also define the reverse graph $\mathcal{G}^\dagger = (\mathcal{E}^\dagger, \mathcal{V}^\dagger)$ where the direction of the edges are reversed but the vertex set remains the same: $\mathcal{V}^\dagger = \mathcal{V}$. Analogous to the definitions in Notation 1.2, let $\Sigma_0^\dagger$ be the empty string $\emptyset$, $\Sigma_k^\dagger$ be the set of directed paths in $\mathcal{G}^\dagger$ of length $k \in \mathbb{N}$, and $\Sigma_\infty^\dagger$ be the set of directed paths of infinite length. Define

$$\Sigma^\dagger := \Sigma_*^\dagger \cup \Sigma_\infty^\dagger \text{ where } \Sigma_*^\dagger := \cup_{k \in \mathbb{N}_0} \Sigma_k^\dagger.$$

Example 1.3. To give the reader something concrete to follow, we introduce an example graph IFS . Let $\mathcal{F} = \{f_1, ..., f_5\}$ be a set of five contractive maps with scaling factor $0 < s < 1$. We do not define explicit maps here but note that the Penrose IFS takes this form. The allowed composition of functions in $\mathcal{F}$ is determined by the graph $\mathcal{G}$ displayed at the left of Figure 1.1. On the right side of the same figure, we display the reverse graph $\mathcal{G}^\dagger$. The vertex set for both of these graphs is $\mathcal{V} = \{a, b\}$. The strings 145314 and 125413 correspond to example directed paths of finite length in $\mathcal{G}$ and $\mathcal{G}^\dagger$ respectively. So by the notation introduced above, $145314 \in \Sigma_*$ and $125413 \in \Sigma_*^\dagger$. We emphasise that Σ and $\Sigma^\dagger$ are subspaces of the code space (see Remark 1.4) that contains all finite and infinite strings made from elements in the set $[5] = \{1, 2, 3, 4, 5\}$.

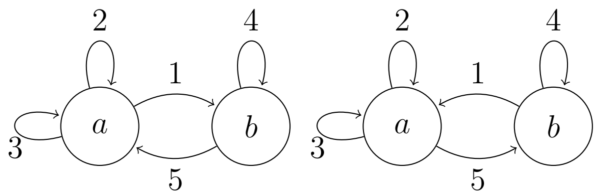

Figure 1.1: Penrose IFS graph $\mathcal{G}$ and reverse graph $\mathcal{G}^\dagger$

Remark 1.4. The structure of code spaces is thoroughly discussed in the fractals literature (see [Bar93] and [Bar06] for example) Set $[N] := \{1, 2, \cdots N\}$, then define $[N]^k$ as the set of strings of length k, $[N]^*$ as the set of strings of finite length and $[N]^\infty$ as the set of strings of infinite length. The space $[N]^* \cup [N]^\infty$ is a code space and can easily be equipped with a metric $d_{[N]^* \cup [N]^\infty}$ such that it becomes a compact metric space [BV17b]. With an induced subspace metric d_Σ, the space Σ, defined for a graph IFS with N maps, is a shift invariant compact subspace of $[N]^* \cup [N]^\infty$. For the shift transformation $S : [N]^* \cup [N]^\infty \to [N]^* \cup [N]^\infty$ which removes the first element of the string, we have that $S|_\Sigma : \Sigma \to \Sigma$ is continuous.

For convenience, we introduce extra notation to represent the composition of functions associated with strings in code space.

Notation 1.5. For $\theta = \theta_1\theta_2 \ldots \theta_k \in \Sigma_*$,

$$f_\theta := f_{\theta_1} f_{\theta_2} \cdots f_{\theta_k}$$
$$f_{-\theta} := f_{\theta_1}^{-1} f_{\theta_2}^{-1} \cdots f_{\theta_k}^{-1} = (f_{\theta_k} f_{\theta_{k-1}} \cdots f_{\theta_1})^{-1}.$$

If $\theta = \emptyset$, f_θ and $f_{-\theta}$ are the identity function. For $\theta \in \Sigma_\infty$ and $k \in \mathbb{N}_0$ let $\theta|k := \theta_1\theta_2 \ldots \theta_k$. For $\theta \in \Sigma$, define the length of θ as

$$|\theta| := \begin{cases} k & \theta \in \Sigma_k \\ \infty & \theta \in \Sigma_\infty. \end{cases}$$

1.2 Attractors and Code Space

Before explaining how to construct tilings from a graph IFS, we review some standard fractal theory on attractors and code space. Let $\mathbb{H}$ be the non-empty compact subsets of $\mathbb{R}^M$. Equipped with the Hausdorff metric, the space $\mathbb{H}$ is complete (see [Bar93, Theorem 7.1] for a proof). Let $\mathbb{H}^V$ be the product of V copies of $\mathbb{H}$.

Definition 1.6. Define $\mathbf{F} : \mathbb{H}^V \to \mathbb{H}^V$ by

$$(\mathbf{F}X)_v := \{x \in f_e X_w \,:\, e \in \mathcal{E}_{w,v}, w \in \mathcal{V}\} \tag{1.1}$$

for all $X \in \mathbb{H}^V$, where X_w is the w^{th} component of X.

Theorem 1.7. *The map $\mathbf{F} : \mathbb{H}^V \to \mathbb{H}^V$ is a contraction. There exists a unique vector of compact sets $\mathbf{A} = (A_1, A_2, ...A_V) \in \mathbb{H}^V$ such that*

$$\mathbf{A} = \mathbf{F}\mathbf{A} \;\; \textit{and} \;\; \mathbf{A} = \lim_{k\to\infty} \mathbf{F}^k \mathbf{B}$$

for all $\mathbf{B} \in \mathbb{H}^V$, where convergence is with respect to the Hausdorff metric on $\mathbb{H}^V$.

Theorem 1.7 summarises the existence of a unique vector of compact sets that is the fixed point of Equation 1.1. This result is well-known in the IFS literature (for example see [MW88, Theorem 1] or [Bar93, Chapter 10]).

Definition 1.8. Define the union of the components of $\mathbf{A}$ as $A := \bigcup_{v\in\mathcal{V}} A_v$. The set $A \in \mathbb{H}$ is called the attractor of the graph IFS and $\{A_v : v \in \mathcal{V}\}$ are its components.

For our purposes, we will always assume that the attractor components do not overlap: $A_i \cap A_j = \emptyset$ for $i \neq j$. If this was not the case, we could apply a change of coordinates to make a new graph IFS that did satisfy this condition [BV18].

Example 1.9. We sketch how to obtain the attractor of an IFS with the form presented in Example 1.3. Following Definition 1.6, for any $X \in \mathbb{H}^2$

$$\begin{aligned}(\mathbf{F}X)_a &= \{x \in f_e X_w \,:\, e \in \mathcal{E}_{w,a},\, w \in \mathcal{V}\} \\ &= \{x \in f_e X_w \,:\, e \in \{1,2,3\}\} \\ &= \{x \in f_1 X_b, x \in f_2 X_a, x \in f_3 X_a, \} \\ (\mathbf{F}X)_b &= \{x \in f_4 X_b, x \in f_5 X_a\}.\end{aligned}$$

By Theorem 1.7, we know there exists $(A, B) \in \mathbb{H}^2$, the unique vector of compact sets, with

$$A = f_1(B) \cup f_2(A) \cup f_3(A) \text{ and } B = f_4(B) \cup f_5(A).$$

Ensuring that the maps were defined such that A and B do not overlap, we call $P := A \cup B$ the attractor of the IFS. Figure 1.2 displays this construction for the Penrose IFS whose maps have scaling factor $\frac{1}{\tau}$ where $\tau = \frac{1+\sqrt{5}}{2}$ is the golden ratio (for explicit maps see [BV14]).

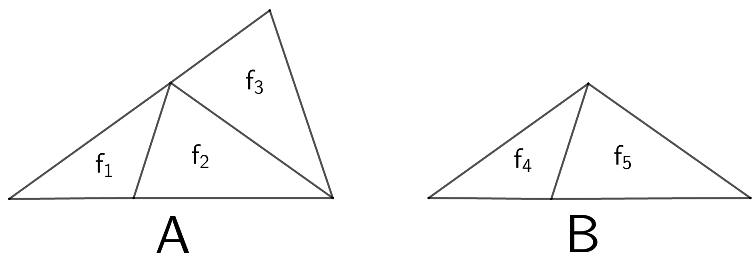

Figure 1.2: Penrose IFS attractor

Definition 1.10. Define $\overrightarrow{v}(i), \overleftarrow{v}(i) \in V$ as the unique vertices such that e_i is the directed edge in $\mathcal{G}$ from $\overleftarrow{v}(i)$ to $\overrightarrow{v}(i)$.

Definition 1.11. The coding map $\pi : \Sigma \to \mathbb{H}(A)$ is defined by

$$\begin{aligned}\pi(\varnothing) &= A, \\ \pi(\omega) &= f_\omega(A_{\overrightarrow{v}(\omega_k)}) \text{ for all } \omega = \omega_1\omega_2 \ldots \omega_k \in \Sigma_*, k \in \mathbb{N} \\ \pi(\sigma) &= \lim_{k\to\infty} \pi(\sigma|k), \text{ for all } \sigma \in \Sigma_\infty,\end{aligned}$$

where the limit is with respect to the Hausdorff metric and $\mathbb{H}(A)$ is the non-empty compact subsets of A.

Theorem 1.12. *The coding map $\pi : \Sigma \to \mathbb{H}(A)$ is well-defined and continuous with respect to the Hausdorff metric. When restricted to Σ_∞, the map π is continuous from Σ_∞ to $\mathbb{R}^M$ and*

$$\pi(\Sigma_\infty) = \{\pi(\sigma) : \sigma \in \Sigma_\infty\} = \cup_{v \in \mathcal{V}} A_v = A$$

The coding map provides an address space structure for the attractor. For a thorough explanation of the relationship between subsets of the attractor and address spaces from this perspective see [Bar06, Chapter 3].

1.3 Tilings

Everything we have introduced so far holds for all graph IFSs. To define a tiling IFS extra conditions are required.

Definition 1.13. Let $\mathcal{F} = \{\mathbb{R}^M; f_1, f_2 \cdots f_N\}$ with $N \geq 2$ and graph $\mathcal{G}$ be a graph IFS of contractive similitudes where for fixed $0 < s < 1$ the scaling factor of each f_i is $\lambda_i = s^{a_i}$ with $a_i \in \mathbb{N}$. Also suppose $\gcd\{a_1, a_2, ...a_N\} = 1$ and define

$$a_{\max} = \max\{a_i : i = 1, 2, ...N\}.$$

For $x \in \mathbb{R}^M$, the function $f_i : \mathbb{R}^M \to \mathbb{R}^M$ is defined by

$$f_i(x) = s^{a_i} O_i(x) + q_i$$

where O_i is an orthogonal linear transformation and $q_i \in \mathbb{R}^M$. Let $D_H(X)$ be the Hausdorff dimension of $X \subset \mathbb{R}^M$. It is required that

$$D_H(f_e(A_{\overrightarrow{v}(e)}) \cap f_l(A_{\overrightarrow{v}(l)})) < D_H(A)$$

for all $e, l \in \mathcal{E}$ with $e \neq l$. Also ensure that $A_i \cap A_j = \emptyset$ for all $i \neq j$. If these conditions are satisfied then $(\mathcal{F}, \mathcal{G})$ is called a tiling IFS.

We focus on drawing the reader's attention to two key requirements in Definition 1.13. Firstly, the maps in the IFS must satisfy an algebraic condition on their scaling factors. All scaling factors must be integer powers of the same fixed $0 < s < 1$. Secondly, the Hausdorff dimension of the overlap of attractor components must be smaller than the Hausdorff dimension of the attractor. For an thorough explanation of Hausdorff dimensions see [Hut81].

When investigating a fractal generated from an iterated function system, one often starts with the attractor and zooms in to see similar copies of the attractor on smaller scales. Instead of zooming in, the construction of tilings is motivated by expanding outwards. The idea is to take the attractor and expand and split it appropriately so that the new larger set is made from scaled copies of the original attractor. This explains why tilings made in this way are often referred to as 'fractal blow-ups'. The scaled copies, associated with strings of maps, are the fractal tiles in the tiling. To make sure the tiles are appropriately sized, we need to keep track of the scaling factors of the maps. Since the maps in a tiling IFS have scaling factors that are integer powers of some fixed $0 < s < 1$, we define ξ and ξ^- as functions on code space whose values are the sum of elements in the set $\{a_1, a_2, ...a_N\}$.

Definition 1.14. For $\sigma = \sigma_1\sigma_2...\sigma_k \in \Sigma_*$, define

$$\begin{aligned}\xi(\sigma) &= a_{\sigma_1} + a_{\sigma_2} + ... + a_{\sigma_k}\\ \xi^-(\sigma) &= a_{\sigma_1} + a_{\sigma_2} + ... + a_{\sigma_{k-1}}\end{aligned}$$

and $\xi(\emptyset) = \xi^-(\emptyset) = 0$. We call $\xi(\sigma)$ the scaling length of σ.

Next, we define sets of strings that start at a specified vertex in the graph and whose scaling length are only just larger than some fixed positive integer value. A key idea captured in a forthcoming proposition is that the elements in this set are in bijective correspondence with tiles in some bounded tilings.

Definition 1.15. For all $k \in \mathbb{N}_0$ and $v \in \mathcal{V}$, define scaling sets as

$$\begin{aligned}\Omega_k^v &= \{\sigma \in \Sigma_* : \xi(\sigma) > k \geq \xi^-(\sigma), \sigma_1 \in \mathcal{E}_{*,v}\},\\ \Omega_k &= \bigcup_{v \in \mathcal{V}} \Omega_k^v = \{\sigma \in \Sigma_* : \xi(\sigma) > k \geq \xi^-(\sigma)\}.\end{aligned}$$

Using these scaling sets, the tiling map Π is defined from directed paths in the reverse graph $\mathcal{G}^\dagger$ to the collection of compact subsets of $\mathbb{H}(\mathbb{R}^M)$ as follows.

Definition 1.16. The tiling map $\Pi : \Sigma^\dagger \to \mathbb{H}(\mathbb{H}(\mathbb{R}^M))$ is

$$\Pi(\theta_1\theta_2...\theta_k) := \{f_{-\theta_1\theta_2...\theta_k}\pi(\sigma) : \sigma \in \Omega^v_{\xi(\theta_1\theta_2...\theta_k)}\}$$

for $\theta \in \Sigma_*^\dagger$, where v is the unique vertex such that θ_k is a directed edge in $\mathcal{G}^\dagger$ to vertex v, and

$$\Pi(\theta) := \bigcup_{k \in \mathbb{N}} \Pi(\theta|k).$$

for $\theta \in \Sigma_\infty^\dagger$.

For convenience, let $\mathbb{T}_* := \Pi(\Sigma_*^\dagger)$ and $\mathbb{T}_\infty := \Pi(\Sigma_\infty^\dagger)$ be the set of tilings made from strings of finite and infinite length respectively. Let $\mathbb{T} := \Pi(\Sigma^\dagger)$ be the union of these sets.

Definition 1.17. The prototile set $\mathcal{P}$ of a tiling T is a minimal set of tiles such that every tile in T is an isometric copy of a tile in $\mathcal{P}$.

Remark 1.18. The image of the tiling map is contained in the space $\mathbb{H}(\mathbb{H}(\mathbb{R}^M))$, the space of compact subsets of the sets of compact subsets of the metric space $(\mathbb{R}^M, d)$ with d the usual Euclidean metric. Thinking of a tiling as a set of tiles, each of which is a compact subset of $\mathbb{R}^M$, it is clear that tilings are points in $\mathbb{H}(\mathbb{H}(\mathbb{R}^M))$.

In [BV18] the authors describe a convenient metric for tiling spaces. Let $\mathcal{U}$ denote the group of isometries of $\mathbb{R}^M$ and fix $\mathcal{T}$ some group contained in $\mathcal{U}$. Also, fix a prototile set $\mathcal{P}$. Define $\mathbb{T}'$ as the set of all tilings on $\mathbb{R}^M$ made from tiles in $\mathcal{P}$ mapped by elements of $\mathcal{T}$. Let $t_\emptyset$ be the empty tile which can be thought of as a tile at infinity. The usual M-dimensional stereographic projection to the M-sphere is denoted $\rho : \mathbb{R}^M \to \mathbb{S}^M$. Define $\hat{\rho} : \mathbb{T}' \to \mathbb{S}^M$ by

$$\hat{\rho}(T) = \{\rho(t) : t \in T, t \neq t_\emptyset\} \cup \hat{\rho}(t_\emptyset)$$

where $\hat{\rho}(t_\emptyset)$ takes $t_\emptyset$ to the top of the sphere diametric to the origin. Let $\mathbb{H}(\mathbb{H}(\mathbb{S}^M))$ be the nonempty compact subsets of the nonempty compact subsets of $\mathbb{S}^M$. By [Bar06, Chapter 1], $(\mathbb{H}(\mathbb{H}(\mathbb{S}^M)), d_{\mathbb{H}(\mathbb{H}(\mathbb{S}^M))})$ is a compact metric space. Then the tiling metric on $\mathbb{T}'$ is defined as

$$d_{\mathbb{T}'}(T_1, T_2) = d_{\mathbb{H}(\mathbb{H}(\mathbb{S}^M))}(\hat{\rho}(T_1), \hat{\rho}(T_2)).$$

The space $(\mathbb{T}', d_{\mathbb{T}'})$ is compact [BV18].

Definition 1.19. A tiling T is quasiperiodic (also called repetitive in the literature) if for any patch P in T there exists a $R_P > 0$ such that any ball of radius R_P contains an isometric copy of P. Two tilings are locally isomorphic if any patch in either tiling also appears in the other tiling.

Definition 1.20. A symmetry of a tiling is an isometry that takes tiles to tiles. A tiling is periodic if there exists a translational symmetry. In other terms, a tiling T, a subset of $\mathbb{R}^M$, is periodic if $T = T + v$ for some $v \in \mathbb{R}^M$. If no non-zero vector $v \in \mathbb{R}^M$ exists, the tiling is called non-periodic.

Definition 1.21. An IFS $(\mathcal{F}, \mathcal{G})$ is purely self-referential if $\mathcal{E}_{v,v} \neq \emptyset$ for all $v \in \mathcal{V}$.

The following theorem, stating properties of tilings in the set $\mathbb{T}$, is presented in [BV18, Theorem 4 and Theorem 6], generalising the results and proofs from [BV17b]. In later sections and chapters we refer to various parts of this theorem as it relates to examples and other results.

Theorem 1.22. *Let $(\mathcal{F}, \mathcal{G})$ be a tiling IFS.*

(a) Each set $\Pi(\theta)$ in $\mathbb{T}$ is a tiling of a subset of $\mathbb{R}^M$, the subset being bounded when $\theta \in \Sigma_*^\dagger$ and unbounded when $\theta \in \Sigma_\infty^\dagger$.

(b) For all $\theta \in \Sigma_\infty^\dagger$, the sequence of tilings $\{\Pi(\theta|k)\}_{k=1}^\infty$ is nested according to

$$\Pi(\theta|1) \subset \Pi(\theta|2) \subset \Pi(\theta|3)...$$

(c) If $(\mathcal{F}, \mathcal{G})$ is purely self-referential, then for all $\theta \in \Sigma^\dagger$, with $|\theta|$ sufficiently large, the prototile set for $\Pi(\theta)$ is

$$\mathcal{P} = \{s^i A_v : i \in \{1, 2, ...a_{max}\}, v \in \mathcal{V}\}.$$

(d) The map

$$\Pi : \Sigma^\dagger \to \mathbb{T} \subset \mathbb{T}'$$

is continuous from the compact metric space $(\Sigma^\dagger, d_{\Sigma^\dagger})$ into the compact metric space $(\mathbb{T}', d_{\mathbb{T}'})$.

(e) Each tiling in $\mathbb{T}_\infty$ is quasiperiodic and each pair of tilings in $\mathbb{T}_\infty$ are locally isometric.

So the tiling map provides an elegant construction of quasiperiodic tilings from infinite strings in code space. In chapter 3, we consider various spaces of tilings and observe that quasiperiodicity alone does not make these spaces interesting. However, when paired with other properties such as non-periodicity the spaces of tilings are very pathological (discussion in section 3.1). For this chapter, we are primarily concerned with tilings in the image of Π. These tilings exhibit a neat nesting property and have a prototile set that is easy to describe. Next, we define a sequence of tilings that group bounded tilings in the image of Π.

Definition 1.23. The sequence of tilings

$$T_k := s^{-k}\pi(\Omega_k) \text{ and } T_k^v := s^{-k}\pi(\Omega_k^v)$$

for $k \in \mathbb{N}$ and $v \in \mathcal{V}$ are called the canonical tilings of the tiling IFS $(\mathcal{F}, \mathcal{G})$.

Theorem 1.24. *For all $\theta \in \Sigma_*^\dagger$,*

$$\Pi(\theta) = E_\theta T_{\xi(\theta)}^{\overrightarrow{v}(\theta_{|\theta|})},$$

for $E_\theta = f_{-\theta} s^{\xi(\theta)}$.

Proof. Writing $\theta = \theta_1 \dots \theta_k$ with $|\theta| = k$, it follows that

$$\begin{aligned}
\Pi(\theta) &= f_{-\theta_1\dots\theta_k}\{\pi(\sigma) : \sigma \in \Omega_{\xi(\theta_1\dots\theta_k)}^{\overrightarrow{v}(\theta_k)}\} \\
&= f_{-\theta_1\dots\theta_k} s^{\xi(\theta_1\dots\theta_k)} s^{-\xi(\theta_1\dots\theta_k)}\{\pi(\sigma) : \sigma \in \Omega_{\xi(\theta_1\dots\theta_k)}^{\overrightarrow{v}(\theta_k)}\} \\
&= E_{\theta_1\dots\theta_k} T_{\xi(\theta_1\dots\theta_k)}^{\overrightarrow{v}(\theta_k)}.
\end{aligned}$$

□

Every bounded tiling is related by isometry to some canonical tiling. We refer back to proof of Theorem 1.24 explicitly in section 5.1 with regards to a similar result in the mixed tiling setting.

Definition 1.25. The relative address of a tile $t \in T_k^v$ is defined as $\emptyset.\pi^{-1}s^k(t) \in \emptyset.\Omega_k^v$.

Relative addresses put an address space structure on the set of canonical tilings. The next proposition follows directly from the definition of T_k and relative addresses since the map $s^{-k}\pi : \Omega_k \to T_k$ is surjective and injective.

Proposition 1.26. *The tiles of T_k are in bijective correspondence with the set of relative addresses $\emptyset.\Omega_k$.*

By Theorem 1.24 every tiling of the form $\Pi(\theta)$ for some $\theta \in \Sigma$ is related by isometry to the canonical tiling $T_{\xi(\theta)}$. Then from Proposition 1.26, it is clear that any tile $t \in \Pi(\theta)$ is also assigned a relative address. To get a feel for address space structures on tilings and the mechanics of the tiling map we discuss two example tiling IFSs.

1.4 Examples

The two example IFSs showcased in this section are the Fibonacci and golden-b. These two systems play a major role in our story since they are among the simplest one and two dimensional examples whose maps have more than a single scaling ratio.

1.4.1 Fibonacci

Let $\mathcal{F} = \{f_1 = sx, f_2(x) = s^2x + s : s + s^2 = 1, s > 0\}$ and $\mathcal{G}$ is a single vertex graph with two loops labelled 1 and 2. We call $(\mathcal{F}, \mathcal{G})$ the Fibonacci IFS. The address space is $[2]^*$ for finite strings and $[2]^\infty$ for infinite strings. Denote the unit interval by I. Since $f_1(I) \cup f_2(I) = I$, the attractor of $\mathcal{F}$ is I. The prototile set is $\{a, b\}$ where $a := sI$ and $b := s^2I$. We call a a large tile and b a small tile. Tiling blow-ups of the form $\Pi(\theta)$ for $\theta \in [2]^*$ look like decorations of intervals on the real line. Using Definition 1.16 we explicitly construct some example bounded tilings. The attractor is tiled by the two tiles in the set $\Pi(\emptyset) = \{f_1(I), f_2(I)\}$ as illustrated in Figure 1.3. Next, consider $\Pi(1) = \{f_{-1}\pi(\theta) : \theta \in \Omega_1\}$ where $\Omega_1 = \{11, 12, 2\}$. So

$$\Pi(1) = \{f_{-1}f_{11}(I), f_{-1}f_{12}(I), f_{-1}f_2(I)\}$$

is a bounded tiling made from three tiles pictured at the top of Figure 1.4. The relative addresses, identified from the set Ω_1 are labelled under each tiling. Since

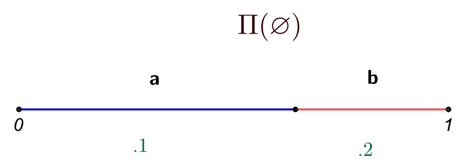

Figure 1.3: Fibonacci tiling $\Pi(\emptyset)$

$\xi(2) > \xi(1)$ we expect the bounded tiling $\Pi(2)$ to have more tiles than $\Pi(1)$. Observe that $\Pi(2) = \{f_{-2}\pi(\theta) : \theta \in \Omega_2\}$ where $\Omega_2 = \{111, 112, 12, 21, 22\}$ so

$$\Pi(2) = \{f_{-2}f_{111}(I), f_{-2}f_{112}(I), f_{-2}f_{12}(I), f_{-2}f_{21}(I), f_{-2}f_{22}(I)\}$$

pictured at the bottom left of Figure 1.4.

The tiling $\Pi(11)$ is pictured to the right of $\Pi(2)$ for comparison. Since $\xi(2) = \xi(11)$, the tilings have the same set of relative addresses but $\Pi(11)$ is translated

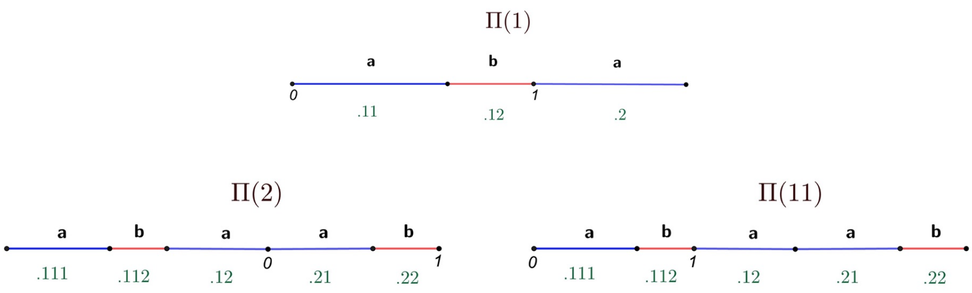

Figure 1.4: Fibonacci tilings Π(1), Π(2) and Π(11)

to the right. Determining when two tilings are translations, or more generally isometries of one another, is a key idea explored in section 2.1.

Often for convenience, we write canonical Fibonacci tilings as strings of the form

$$\begin{aligned} T_0 &= ab \\ T_1 &= aba \\ T_2 &= abaab \\ T_3 &= abaababa \\ T_4 &= abaababaabaab \end{aligned}$$

where a is the big tile and b is the small tile.

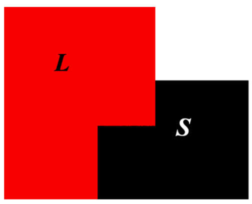

Figure 1.5: Golden-b attractor

1.4.2 Golden-B

Just like the Fibonacci IFS, the golden-b IFS has two maps $\mathcal{F} = \{f_1, f_2\}$ with scaling ratios s and s^2. In this case, the ratio satisfies $s^2 + s^4 = 1$ and the maps are

$$f_1\begin{pmatrix}x\\y\end{pmatrix}=\begin{pmatrix}0 & s\\-s & 0\end{pmatrix}\begin{pmatrix}x\\y\end{pmatrix}+\begin{pmatrix}0\\s\end{pmatrix} \text{ and } f_2\begin{pmatrix}x\\y\end{pmatrix}=\begin{pmatrix}-s^2 & 0\\0 & s^2\end{pmatrix}\begin{pmatrix}x\\y\end{pmatrix}+\begin{pmatrix}1\\0\end{pmatrix}.$$

The attractor is the hexagon $G \in \mathbb{R}^2$ which is the only rectilinear polygon that can be tiled by two different scaled copies of itself [BV17b]. We define $L := f_1(G)$ the large tile and $S := f_2(G)$ the small tile (see Figure 1.5). The golden-b IFS has an identical addresses space to the Fibonacci IFS: $[2]^*$ for finite strings and $[2]^\infty$ for infinite strings. Figure 1.6 shows the bounded tilings $\Pi(1), \Pi(2)$ and $\Pi(11)$. Figure 1.7 depicts the first 4 canonical tilings with their relative addresses labelled.

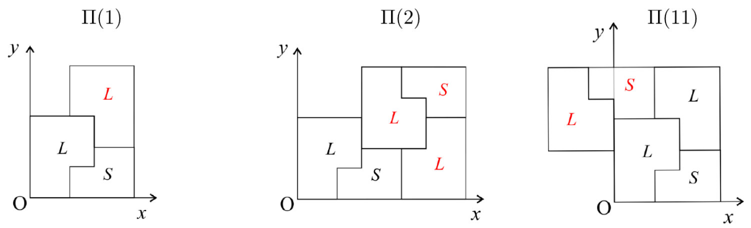

Figure 1.6: Golden-b $\Pi(1), \Pi(2)$ and $\Pi(11)$ tilings [BV17b]

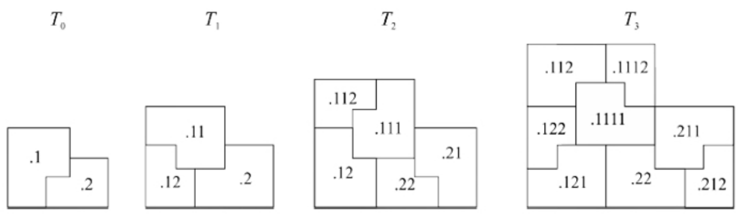

Figure 1.7: Golden-b canonical tilings [BV17b]

Chapter 2

Local Rigidity

This chapter explains some consequences when a tiling IFS is 'locally rigid'. Importantly, when a tiling IFS satisfies this condition it admits an invertible inflation map. The existence of an invertible inflation map is a key requirement for the tiling systems considered by Anderson and Putnam [AP98]. We explore how the symbolic tiling theory connects to the Anderson and Putnam theory in chapter 3.

In this chapter, we primarily follow [BV18] and remain in the symbolic tiling realm, examining tilings in the image of the tiling map Π. In section 2.1 we define 'local rigidity' and showcase some neat consequences for the canonical sequence of tilings and tilings in the set $\mathbb{T}$. Section 2.2 describes how to construct an invertible inflation map. Finally, in section 2.3 we present two more example tiling IFSs whose tilings are made from tiles with no interiors.

2.1 Definition and Consequences

Definition 2.1. Suppose $(\mathcal{F}, \mathcal{G})$ is a graph IFS. Let $\mathcal{T}$ be the group of isometries generated by the set of maps in $\mathcal{F}$ and $\mathcal{U}$ be the group of all isometries on $\mathbb{R}^M$. Let $\mathcal{T}' \subset \mathcal{T}$ be the groupoid of isometries of the form $f_{-\theta} f_\sigma$ where $\sigma \in \Sigma_*$, $\theta \in \Sigma_*^\dagger$ and $\overleftarrow{v}(\sigma_1) = \overrightarrow{v}(\theta_{|\theta|})$. For $\theta \in \Sigma_*$, we define the isometry $E_\theta := f_{-\theta} s^{\xi(\theta)}$.

Definition 2.2. The tiling IFS $(\mathcal{F}, \mathcal{G})$ is called locally rigid when the following two conditions hold:

(i) If $E \in \mathcal{T}'$, $v \in \mathcal{V}$ with $T_0^v \cap ET_0^v \neq \emptyset$ then $E = id$.

(ii) If $E \in \mathcal{T}$ such that $T_0^v \cap ET_0^w$ tiles $A_v \cap EA_w$ for some $v, w \in \mathcal{V}$ then $E = id$ and $v = w$.

Theorem 2.3. *If $\mathcal{F} = \{f_n : n \in [N]\}$ has non-isometric tiles, then it is locally rigid.*

Proof. Since $|\mathcal{V}| = 1$ we only need to check condition (i) from Definition 2.2. Suppose for some $E \in \mathcal{T}'$, we have $T_0 \cap ET_0 \neq \emptyset$. Because the tiles are non-isometric, there must exist $n \in [N]$ such that $f_n(A) = Ef_n(A)$. Since $E = f_{-\theta}f_\omega$ for some $\theta, \omega \in [N]^*$, we have that $f_\theta f_n(A) = f_\omega f_n(A)$. Hence, $\theta n = \omega n$ and so $\theta = \omega$. It follows that $E = f_{-\theta}f_\theta = id$. □

Example 2.4. Since the golden-b and Fibonacci attractors are tiled by two non-isometric tiles, it follows as a corollary from Theorem 2.3 that they are both locally rigid. We can also see that the golden-b and Fibonacci are locally rigid IFSs by inspecting the images of their corresponding attractors (Figures 1.5 and 1.3). By trying to rotate and flip the golden-b attractor in various ways, it becomes clear that there is no isometry that maps one tile in T_0 to itself that does not also map the other tile to itself. For the Fibonacci IFS, the only way for an isometry to make a non-trivial tileable intersection of two copies of T_0 would be if it involved a reflection. However, this is not possible since the group $\mathcal{T}'$ for the Fibonacci IFS is contained within the group of translations.

Definition 2.5. Recall that for any $\sigma \in \Sigma_*$ the scaling length of σ is defined as $\xi(\sigma)$. For $k \in \mathbb{N}$ and $v \in \mathcal{V}$, we define a subset of the scaling set as

$$\Lambda_k^v = \{\sigma \in \Sigma_* : \xi(\sigma) = k, \overleftarrow{v}(\sigma_1) = v\} \subset \Omega_{k-1}^v,$$

which contains all strings with scaling length k starting at vertex v.

Supposing the IFS is locally rigid, there is a nice relationship between the copies of T_0^v in some larger canonical tiling T_k and strings in the set Λ_k^v. We state without proof this correspondence in the proposition below (see [BV18, Theorem 8]).

Proposition 2.6. *Suppose $\mathcal{F}$ is locally rigid. There is a bijective correspondence between Λ_k^v and the set of copies $ET_0^v \subset T_k$ with $E \in \mathcal{T}$.*

Example 2.7. We consider this correspondence using the golden-b IFS. Recall from section 1.4.2 that the golden-b IFS has address space $[2]^* \cup [2]^\infty$. So the corresponding set for scaling length 3 is

$$\Lambda_3 = \{111, 12, 21\}.$$

Figure 2.1 shows that there are three copies of T_0 in T_3 (as expected from Proposition 2.6) with relative address pairs $\{(.1111, .1112), (.121, .122), (.211, .212)\}$. Moreover, from Theorem 1.24 we know there exists exactly three bounded tilings in the image of the tiling map Π that are related by isometry to T_3. Since the attractor $\Pi(\emptyset)$ must be nested in $\Pi(\theta)$ for any $\theta \in [2]^*$, the three strings in Λ_3 correspond to the possible placement of the attractor at the origin. Figure 2.2 compares the placement of $\Pi(\emptyset)$ in the bounded tilings $\Pi(111)$, $\Pi(12)$ and $\Pi(21)$.

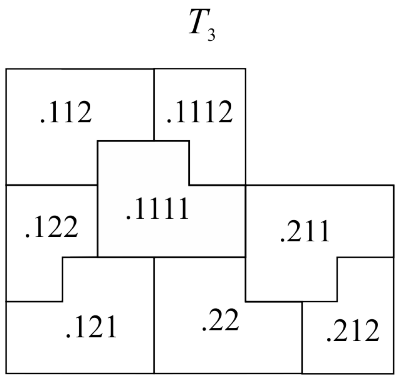

Figure 2.1: Golden-b T_3 canonical tiling

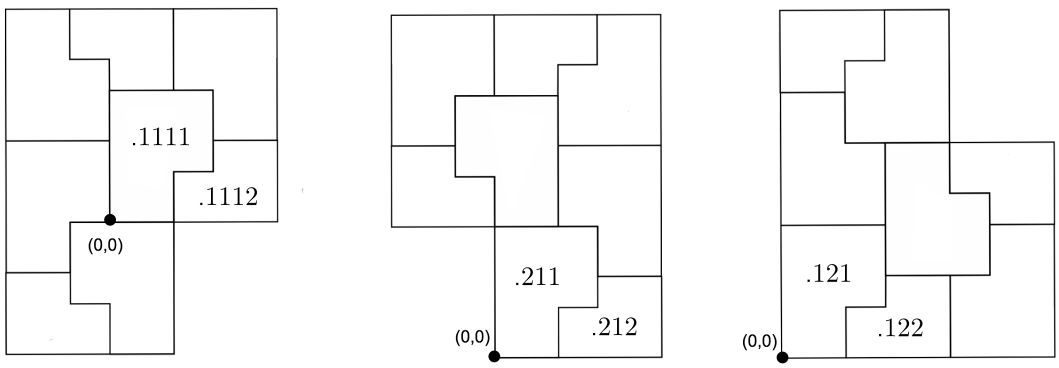

Figure 2.2: Nesting of $\Pi(\emptyset)$ in $\Pi(111)$, $\Pi(12)$ and $\Pi(21)$

Theorem 2.8. *Let $(\mathcal{F}, \mathcal{G})$ be locally rigid. For some $\theta, \psi \in \Sigma^\dagger$ and $E \in \mathcal{T}$, $\Pi(\theta) = E\Pi(\psi)$ if and only if $\exists\, p, q \in \mathbb{N}_0$ such that $\xi(\theta|p) = \xi(\psi|q)$, $E = E_{\theta|p}E^{-1}_{\psi|q}$, $S^p\theta = S^q\psi$ and $\overrightarrow{v}(\theta|p) = \overrightarrow{v}(\psi|q)$.*

Theorem 2.8 is the core result in [BV18] showing that when an IFS is locally rigid it is possible to determine exactly when two tilings (bounded or unbounded) are related by an isometry in $\mathcal{T}$. The proof of the theorem uses Proposition 2.6 and related results (see [BV18, Theorem 9]).

Corollary 2.9. *If $(\mathcal{F}, \mathcal{G})$ is locally rigid, then $\Pi(\theta) = E\Pi(\theta)$ for $E \in \mathcal{T}$ if and only if $E = id$.*

Corollary 2.9 shows that tilings generated from a locally rigid IFS have a similar property to being non-periodic. Instead of requiring that no translation vector maps the tiling to itself, the corollary shows that tilings in the image of Π have the property that no isometry from the group $\mathcal{T}$ maps the tiling to itself. It turns out that many locally rigid IFSs do generated tilings that are non-periodic in the translational sense (discussed in section 3.1).

2.2 Inflation and Deflation

This section explains how a locally rigid IFS admits a well-defined invertible inflation map.

Definition 2.10. Define $\mathbb{Q} := \{ET : E \in \mathcal{T}, T \in \mathbb{T}\}$ and $\mathbb{Q}' := \{ET : E \in \mathcal{T}, T \in \mathbb{T}, T \neq T_0^v$ for any $v \in \mathcal{V}\}$.

Definition 2.11. A bounded tiling $P \in \mathbb{Q}$ is called a partner if $P = ET_0^v$ for some $E \in \mathcal{T}, v \in \mathcal{V}$. For $Q \in \mathbb{Q}$, define Q_P to be the set of all partners in Q. A tile that is isometric to sA_v for some $v \in \mathcal{V}$ is called a large tile. For $Q \in \mathbb{Q}$, define Q_L to be the set of large tiles Q.

Definition 2.12. The amalgamation and shrink operation $\alpha : \mathbb{Q}' \to \mathbb{Q}$ is defined by

$$\alpha Q' = \{st : t \in Q' \setminus Q'_P\} \cup \bigsqcup \{sEA_v : E \in \mathcal{T}, ET_0^v \subset Q'_P, v \in \mathcal{V}\}.$$

The expansion and splitting operation $\alpha^{-1} : \mathbb{Q} \to \mathbb{Q}$ is defined by

$$\alpha^{-1} Q = \{s^{-1}t : t \notin Q_L\} \cup \bigsqcup \{sET_0^v : E \in \mathcal{T}, sEA_v \in Q, v \in \mathcal{V}\}.$$

The amalgamation and shink operation α identifies all tiles that are not in a partner set and shrinks them by a factor s. For tiles in a partner set, the operation joins them together to form a new large tile. The expansion and subdivision operation α^{-1} splits large tiles and expands all other tiles by a factor s^{-1}.

Observe that $\mathbb{Q}'$ is defined as a subset of $\mathbb{Q}$ without tilings isometric to canonical tilings T_0^v for some $v \in \mathcal{V}$. For tilings isometric to something of the form T_0^v, an amalgamation and shrinking process would map outside the set $\mathbb{Q}$. This is a small technical point explaining why the map α has domain $\mathbb{Q}'$.

Proposition 2.13. *If $(\mathcal{F}, \mathcal{G})$ is locally rigid, then α and α^{-1} are well-defined. In particular, $\alpha T_k = T_{k-1}$ and $\alpha^{-1} T_{k-1} = T_k$ for all $k \in \mathbb{N}$.*

The key idea for Proposition 2.13 (see [BV18, Theorem 10]) is that if the IFS is locally rigid we can unambiguously identify partner sets so that the operations α and α^{-1} are well-defined. Consider the partial golden-b tiling in Figure 2.1. It is unambiguous how to match a small tile to a big tile. Note that in both the golden-b and Fibonacci examples only big tiles can exist without partners.

Proposition 2.14. *Suppose $(\mathcal{F}, \mathcal{G})$ is locally rigid, then for all $\theta \in \Sigma_\infty^\dagger$, $n \in [N]$,*

$$\alpha^{a_{\theta_1}} E_{\theta_1}^{-1} \Pi(\theta) = \Pi(S\theta) \text{ and } E_n \alpha^{-a_n} \Pi(\theta) = \Pi(n\theta).$$

Proposition 2.14 (see [BV18, Theorem 11]) captures the conjugacy relation between the operations α and α^{-1}, together with an isometry action, on tilings and the shift and adjoin operations on code space. So applying the shift operation to remove the first element of the string corresponds to applying an isometry and then amalgamating and shrinking (a number of times) the tiling. In contrast, adding an element to the front of the string corresponds to expanding and subdividing (a number of times) and then applying an isometry to the tiling.

On canonical tilings, α and α^{-1} serve as an appropriate inflation and deflation pair. For tilings $\Pi(\theta)$ with $\theta \in \Sigma^\dagger$, if we want the inflation and deflation operations to keep the tiling in the image of Π, Proposition 2.14 gives us the appropriate constructions.

2.3 More Examples

Here we introduce two other protagonists to our story: Sierpinski and rigid Williams. The Sierpinski IFS serves as a canonical example in the fractals literature (see [Man83, Bar93] for example). While the Sierpinski IFS is not locally rigid, the recently uncovered rigid Williams, as the name suggests, is locally rigid.

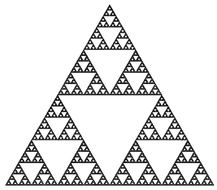

Figure 2.3: Sierpinski attractor

2.3.1 Sierpinski

Let $\mathcal{F} = \{f_1, f_2, f_3\}$ be the Sierpinski IFS with maps

$$f_1 \begin{bmatrix} x \\ y \end{bmatrix} = \begin{bmatrix} \frac{1}{2} & 0 \\ 0 & \frac{1}{2} \end{bmatrix} \begin{bmatrix} x \\ y \end{bmatrix}$$

$$f_2 \begin{bmatrix} x \\ y \end{bmatrix} = \begin{bmatrix} \frac{1}{2} & 0 \\ 0 & \frac{1}{2} \end{bmatrix} \begin{bmatrix} x \\ y \end{bmatrix} + \begin{bmatrix} \frac{1}{2} \\ 0 \end{bmatrix}$$

$$f_3 \begin{bmatrix} x \\ y \end{bmatrix} = \begin{bmatrix} \frac{1}{2} & 0 \\ 0 & \frac{1}{2} \end{bmatrix} \begin{bmatrix} x \\ y \end{bmatrix} + \begin{bmatrix} \frac{1}{4} \\ \frac{\sqrt{3}}{4} \end{bmatrix}.$$

The attractor A is the Sierpinski triangle displayed in Figure 2.3. It is clear that $T_0 \cap ET_0$ tiles $A \cap EA$ for any $E = f_i f_j^{-1}$ with $i \neq j$. Figure 2.4 shows this for the case when $i = 2$ and $j = 1$ with the tileable intersection shaded red. In a Sierpinski blow-up, it is impossible to uniquely identify partners. All the unbounded tilings are periodic, in contrast to the tilings in the next example.

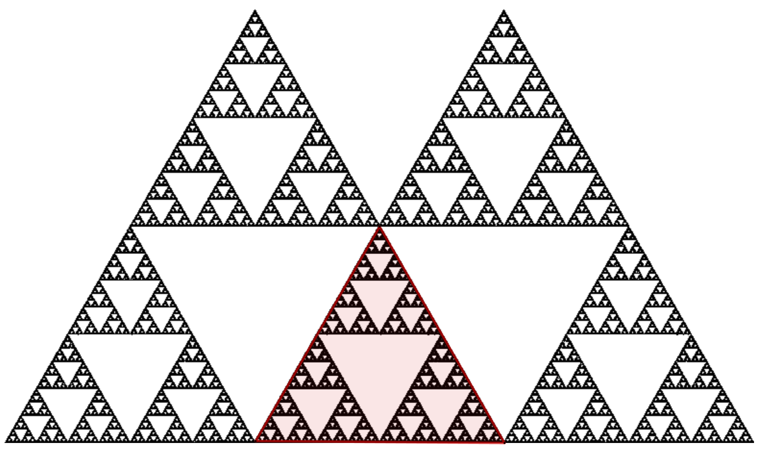

Figure 2.4: Sierpinski tileable overlap

2.3.2 Rigid Williams

In their recent paper [SW18], Steemson and Williams describe the family of generalised Sierpinksi triangles which consists of four types: $\triangle NNN$, $\triangle FNN$, $\triangle FFN$, $\triangle FFF$. The names of the types indicate the orientation, flip or non-flip, of the three maps in the IFS. For example, the Sierpinski IFS from section 2.3.1 has type $\triangle NNN$. The $\triangle FFF$ is the well-known pedal triangle (see [ZHWD08] for example). Steemson and Williams give the first detailed description of the two other members: $\triangle FNN$ (the Steemson) and $\triangle FFN$ (the Williams). Assuming one of the sides has length 1, a general Williams triangle has the form displayed in Figure 2.5.

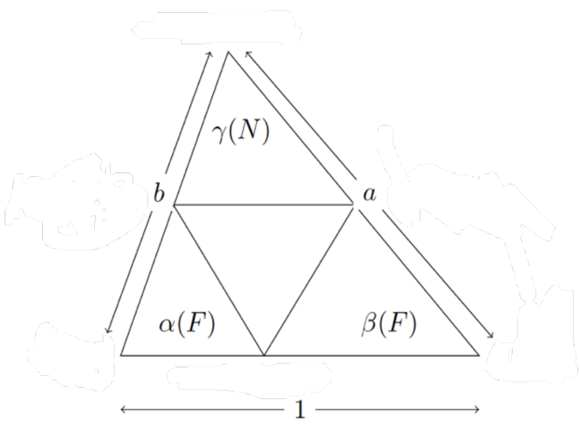

Figure 2.5: General Williams fractal triangle [SW18]

The rigid Williams IFS has scaling factors $\alpha = s$ and $\beta = \gamma = s^2$. The side lengths of the rigid Williams attractor must satisfy the equations:

$$sb + s^2 a = 1$$

$$s + s^2 b = b$$

$$s^2 + s^2 a = a$$

Solving we find $a = \frac{s^2}{1-s^2}$, $b = \frac{s}{1-s^2}$ and $2s^2 + s^4 = 1$. Then $s = \sqrt{\sqrt{2} - 1} \approx 0.644$, $a \approx 0.707$, $b \approx 1.10$. The explicit maps f_1, f_2, f_3 for the IFS can be computed using the methods described in [SW18]. The attractor of the rigid Williams IFS is displayed in Figure 2.6.

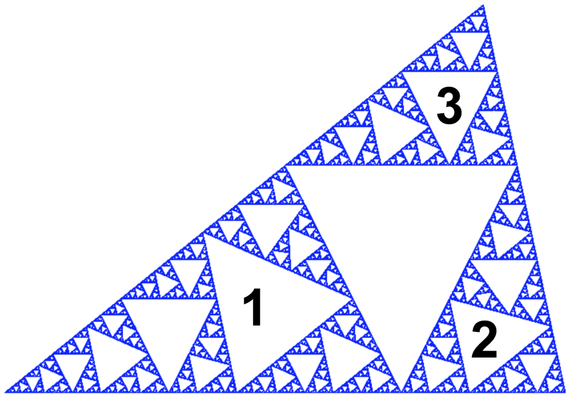

Figure 2.6: Rigid Williams attractor

Under any isometry in $\mathcal{T}$, the tiles can appear in one of six orientations of the attractor. These six possible orientations, three non-flip and three flip, are displayed in Figure 2.7. The idea is that we cannot intersect any of these fractal triangles so that their intersection is non-trivial and tileable. Hence, the IFS is locally rigid. For any tiling blow-up generated from the map $\Pi : [3]^* \cup [3]^\infty \to \mathbb{T}$, we can unambiguously identify partners and apply an amalgamation and shrink operation.

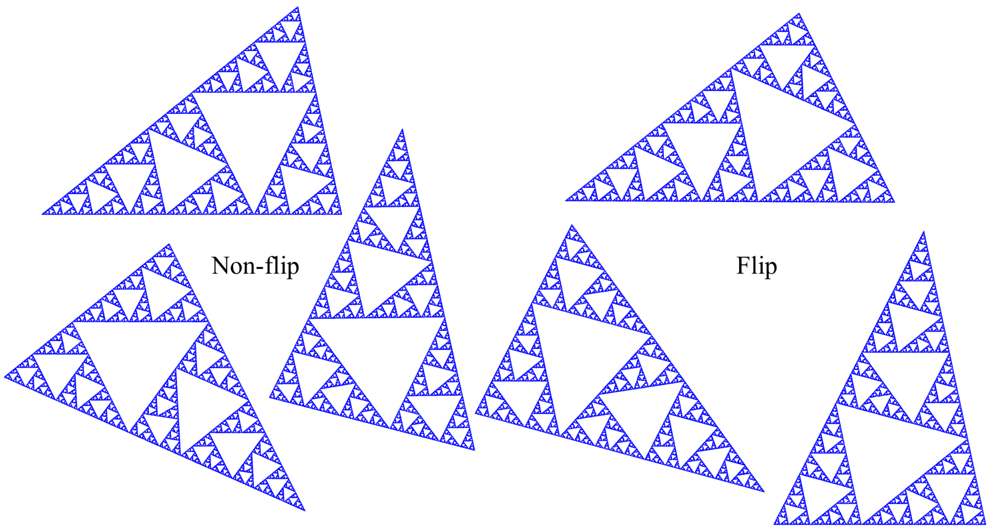

Figure 2.7: Rigid Williams orientations

Chapter 3

Anderson-Putnam Theory

This chapter links the fractal tiling theory outlined in the previous two chapters to mainstream tiling literature. A keystone paper in the tiling literature is by Anderson and Putnam (A & P) which shows how to describe a substitution tiling space in terms of an inverse limit space [AP98]. In section 3.1, we introduce the substitution tiling systems considered by A & P and prove that it is possible to interpret these systems in the tiling IFS framework. However, we emphasise that the tiling IFS theory is more general and not restricted to tiles being homeomorphic to disks or the action being solely contained within the group of translations. The advantage of introducing the A & P tiling perspective is that it has been thoroughly developed and widely applied to compute many things such as the cohomology of tiling spaces. In sections 3.2 and 3.3 we explain the A & P inverse limit construction and use this theory to present the well-known computations of the golden-b and Fibonacci cohomology groups.

3.1 Substitution tiling systems

We introduce substitution tiling systems in the style of [AP98] but slightly change notation and terminology to align with other material in this thesis. To A & P a tile is a subset of $\mathbb{R}^M$ that is homeomorphic to a closed ball in $\mathbb{R}^M$. A partial tiling is a collection of tiles in $\mathbb{R}^M$ with pairwise disjoint interiors and its support is the union of its tiles. A tiling is a partial tiling with support $\mathbb{R}^M$. Let $\mathcal{P} = \{p_i : i \in \{1 \cdots n\}\}$ be a finite prototile set. Let $\hat{\Delta}$ be the collection of all partial tilings that only contain translations of these prototiles. Assume there exists an inflation constant $\lambda > 1$ and a substitution rule that associates to each prototile p_i a partial tiling P_i with support p_i such that λP_i is in $\hat{\Delta}$. The inflation map $\hat{\omega} : \hat{\Delta} \to \hat{\Delta}$ is defined by

$$\hat{\omega}(T) = \lambda \bigcup_{p_i+u\in T} (P_i + u).$$

Let Δ be the collection of tilings in $\hat{\Delta}$ such that for any patch $P \subseteq T$ with bounded support, $P \subseteq \hat{\omega}^n(\{p_i + u\})$ for some $n \in \mathbb{N}$, prototile p_i and vector $u \in \mathbb{R}^M$. Let $\omega = \hat{\omega}|_\Delta$, then the pair (Δ, ω) is the space of tilings and inflation map studied by A & P.

Proposition 3.1. *Any A & P tiling system (Δ, ω) can be expressed as a tiling IFS.*

Proof. Suppose (Δ, ω) is an A & P tiling system with prototile set $\mathcal{P} = \{p_i : i \in \{1 \cdots n\}\}$ and inflation constant $\lambda > 1$. We define a graph IFS $(\mathcal{F}, \mathcal{G})$ such that the number of vertices in $\mathcal{G}$ is the same as the number of prototiles: $V = |\mathcal{V}| = |\mathcal{P}|$. Denote the vertices $\mathcal{V} = \{v_1, \cdots v_n\}$. We know that each prototile p_i is associated with a partial tiling P_i. The tiles in this partial tiling correspond to contractive maps in $\mathcal{F}$ that take various attractor components of the IFS to the attractor component corresponding to the vertex i in $\mathcal{G}$. That is

$$A_{v_i} = \{x \in f_e A_w : e \in \mathcal{E}_{w,v_i}, w \in \mathcal{V}\}.$$

The set of maps constructed in this way for the partial tilings of all prototiles, together with a directed graph that describes which maps take which prototiles into which, fully defines $(\mathcal{F}, \mathcal{G})$. □

It is not true that every tiling IFS can be expressed as an A & P tiling system. Firstly, the tiles in a tiling IFS are not necessarily homeomorphic to disks as we observed with the Sierpinski and rigid Williams tilings in sections 2.3.1 and 2.3.2. Even if the tiles are homeomorphic to disks, it is not always possible to create a finite prototile set such that every tile is a translation of some prototile. A well-known example is the pinwheel tiling [CR98] and in section 5.3 we discuss a new interesting example from [BMT18]. However, in many cases we can expand the prototile set of a tiling IFS to create a new tiling IFS that does fit the A & P setting. We show that this is possible for the golden-b IFS.

3.1.1 Substitution golden-b IFS

In section 1.4.2, we defined the golden-b IFS by $\mathcal{F} = \{f_1, f_2\}$ and let $\{S, L\}$ be the two element prototile set. As in Definition 2.1, let $\mathcal{T}$ be the group generated by the set of isometries that map the prototile set to the tiles in $\mathbb{T}$. By considering compositions of these isometries, we observe that in any tiling there are exactly four possible orientations for S and four orientations for L. Any tile in any tiling in $\mathbb{T}$ is up to translation one of the tiles in the set $\{A, B, C, D, E, F, G, H\}$ displayed in Figure 3.1.

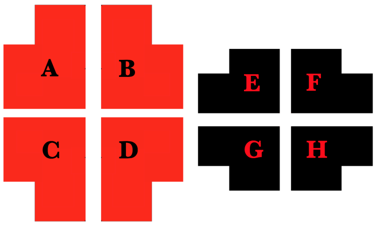

Figure 3.1: Substitution golden-b prototile set

We build a second golden-b IFS whose prototile set is the set of these eight tiles. An appropriate inflation map is constructed by applying α^{-1} twice so that the new large and small tiles in the subdivision have appropriate orientations. By expanding and splitting twice, the small tiles are subdivided into one small and one large tile, while the large tiles are subdivided into one small and two large tiles. Figure 3.2 shows the subdivision for prototiles A and E.

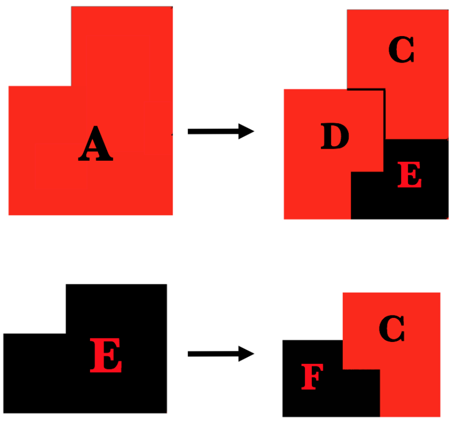

Figure 3.2: Subdivision for prototiles A and E

The new IFS has the form $\tilde{\mathcal{F}} = \{f_1, ...f_{20}\}$ with the 20 maps corresponding to the directed edges in the graph $\tilde{\mathcal{G}}$. The graph $\tilde{\mathcal{G}}$, displayed in Figure 3.3, has eight vertices corresponding to the eight prototiles. Let $\tilde{\mathcal{T}}$ denote the isometries generated by the set of maps in $\tilde{\mathcal{F}}$. Then in this case, $\tilde{\mathcal{T}}$ is a subgroup of the group of translations. Additionally, it is easy to check that this IFS is still locally rigid. Hence, $(\mathcal{F}, \mathcal{G})$ and $(\tilde{\mathcal{F}}, \tilde{\mathcal{G}})$ provide two different address space structures for

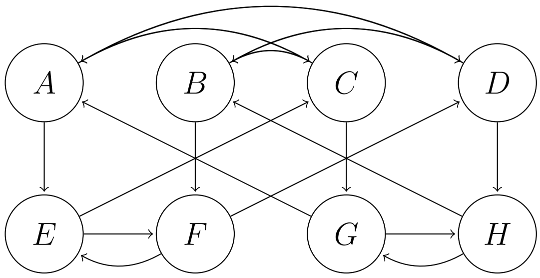

Figure 3.3: Substitution golden-b IFS graph

the same system of tilings. The second IFS is an example of what we now define as a substitution IFS.

Definition 3.2. Let the tiling IFS $(\mathcal{F}, \mathcal{G})$ be called a substitution IFS if the number of vertices in $\mathcal{G}$ correspond to the number of prototiles and $\mathcal{T}$ is contained in the group of translations. Define $\Delta = \{\Pi(\theta) + n : \theta \in \Sigma_{\infty}^{\dagger}, n \in \mathbb{R}^M\}$ and let $\omega = \alpha^{-N}$ with $N \in \{1, ...a_{\max}\}$ be the smallest integer so that $\omega(p)$ is tiled by translations of the prototile set for any $p \in \mathcal{P}$. Then ω is called the inflation map for Δ.

Observe that all tilings in Δ are not necessarily in the image of Π. More specifically, Δ is the closure of $\mathbb{T}_{\infty}$ under the action of translation. We have overloaded the notation Δ and ω in Definition 3.2 to match the space of tilings and inflation map considered by A & P. We believe that these systems are very similar, if not identical. Now we have a way to express these ideas using the tiling IFS framework.

3.1.2 Space of Tilings

In their paper, A & P require that the space of tilings Δ satisfies three conditions [AP98]. We consider what these mean in the IFS setting.

- Firstly, they assume that the tiling inflation map is one-to-one. Recall from section 2.3, that local rigidity makes α and α^{-1} into well-defined inverse operations. Hence, this condition is ensured if the IFS is locally rigid. It is well known that if the inflation map is one-to-one then Δ contains no periodic tilings (see [AP98, Proposition 2.3] for a short proof).

- Secondly, they assume that the substitution is primitive: there is a fixed positive integer N_0 such that for each pair of prototiles p_i and p_j, the partial tiling $\hat{\omega}^{N_0}(\{p_i\})$ contains a translation of p_j. In the IFS setting, this is covered by the condition that the graph is strongly connected.

- Thirdly, they require that the space of tilings satisfies a finite pattern condition: for any $r > 0$ there are only finitely many partial tilings up to translations that are subsets of the tiling space and whose supports have diameters less than r. If we replace the requirement by 'only finitely many partial tilings up to isometry in $\mathcal{T}$' then all tilings from a tiling IFS satisfy this constraint. This is evident by the existence of the canonical tiling sequences. The examples that can be expressed as substitution IFS satisfy the stronger finite pattern condition with the translational requirement.

Remark 3.3. A & P put a metric on the space of tilings Δ by saying that two tilings are close if they almost agree on a large ball about the origin. They formally define the metric d for $T, T' \in \Delta$ by

$$d(T,T') = \inf(\{\frac{1}{\sqrt{2}}\cup\{\,\epsilon \,|\, T+u \text{ and } T+v \text{ agree on } B_{\frac{1}{\epsilon}}(0) \text{ for some } ||u||,||v|| < \epsilon\})$$

with $||\cdot||$ the usual norm on $\mathbb{R}^M$ and $B_r(x)$ an open ball with radius r centred at x. An argument by [RW92] shows that (Δ, d) is a compact metric space.

Using a metric equivalent to the one stated above, many researchers in the tiling community consider spaces that are the completion of the orbit of some tiling T. These spaces are denoted by X_T and called the continuous hull of T. The idea is that if T has some nice properties then X_T also has nice properties. The next theorem states some well-known results about X_T that are thoroughly discussed with appropriate references in [Sad05].

Theorem 3.4. *Let X_T be the continuous hull of a tiling T.*

(a) The tiling space X_T is compact if and only if T satisfies the finite pattern condition.

(b) If T is quasiperiodic then the orbit of every $S \in X_T$ is dense in X_T.

(c) If T is quasiperiodic and non-periodic then X_T locally looks like a disk crossed with a Cantor set.

For the reader familiar with the language of dynamical systems, part (b) means that X_T viewed as a dynamical system by the action of translation is minimal. A & P show that the tiling spaces they consider are always minimal in this sense (see [AP98, Corollary 3.5]). This result has the important consequence that the space of tilings Δ is the same as the closure of the orbit of a single tiling by the translational action, i.e. the spaces X_T described in [Sad05]. Part (c) tells us that when the tilings are quasiperiodic and non-periodic the topology of these tiling spaces is highly pathological. The spaces are connected but not path connected. It is also important for the reader to appreciate that there are two different but closely related dynamical systems at play here. Both involve the space Δ but one is associated with the invertible inflation operation ω and the other is associated with the action of $\mathbb{R}^M$ by translation.

Definition 3.5. Two dynamical systems (Δ_a, ω_a) and (Δ_b, ω_b) are topologically conjugate if there exists a homeomorphism $\pi : \Delta_a \to \Delta_b$ such that $\omega_a = \pi^{-1}\omega_b\pi$.

One of the main contributions of A & P is showing that the dynamical system (Δ, ω) is topologically conjugate to an inverse limit system. To show this topological conjugacy, they construct a CW-complex built from the prototiles of the tiling. The substitution map induces a map from the CW-complex to itself and the inverse limits of such systems turns out to be homeomorphic to the space of tilings. From such a homeomorphism, they show how to calculate cohomology, K-theory and zeta functions for the space of tilings. We narrow our focus to only the first of these computations. Calculating the cohomology of tiling spaces is wide-spread (see [BD08, Sad08] for example) and serves as an important motivation for investigating mixed tiling systems (discussed in section 5.2).

3.2 Forces its Border

For a tiling space Δ to be homeomorphic to an inverse limit space A & P require that the tilings satisfy a condition known as 'forces its border' [AP98].

Definition 3.6. A substitution forces its border if the following condition holds: there is a fixed positive integer M such that for any tile t and any two tilings $T, T' \in \Delta$ both containing t then $\omega^M(T)$ and $\omega^M(T')$ coincide on $\omega^M(\{t\})$ and all tiles that border $\omega^M(\{t\})$.

Example 3.7. For example, the golden-b forces its border. Let $(\tilde{\mathcal{F}}, \tilde{\mathcal{G}})$ be the golden-b substitution tiling IFS and Δ the corresponding space of tilings closed under translations. For $\omega = \alpha^{-2}$ and any tile t, the inflation $\omega^4(\{t\})$ in two separate tilings containing t will agree on all bordering tiles [AP98]. However, we show in the next section that the Fibonacci tiling does not force its border.

A & P's idea was to construct a compact CW-complex Γ_0 by glueing together prototiles in all ways in which the substitution rule allows them to be neighbouring. This is formalised by the definition below.

Definition 3.8. Let $\Gamma_0 = (\Delta \times \mathbb{R}^d)/\sim$ be the product space with the equivalence $(T_1, u_1) \sim (T_2, u_2)$ if tiles t_1 and t_2 with $u_1 \in t_1 \in T_1$ and $u_2 \in t_2 \in T_2$, satisfy $t_1 - u_1 = t_2 - u_2$. The equivalence class of a point (T, u) is denoted $(T, u)_0$.

This equivalence relation identifies two tilings T_1 and T_2 with specified vectors u_1 and u_2 if the vectors lie in the same prototile up to translation.

Proposition 3.9. *The inflation map ω induces a continuous map γ_0 from Γ_0 onto Γ_0 defined by $\gamma_0((T, u)_0) = (\omega(T), \lambda u)_0$.*

Definition 3.10. Let $\Delta_0 = \varprojlim \Gamma_0$ be the inverse limit relative to the bonding map γ_0. This means Δ_0 consists of all infinite sequences $\{x_i\}_{i=0}^{\infty}$ of points in Γ_0 such that $\gamma_0(x_i) = x_{i-1}$. Then a right shift map $\omega_0 : \Delta_0 \to \Delta_0$ is defined by $\omega_0(x)_i = \gamma_0(x_i)$. The map ω_0 is a homeomorphism and (Δ_0, ω_0) is a dynamical system.

Proposition 3.11. *If the substitution tiling forces its border then the dynamical systems (Δ, ω) and (Δ_0, ω_0) are topologically conjugate.*

For complete proofs of Proposition 3.9 and 3.11 we direct the reader to [AP98, Proposition 4.2 and Theorem 4.3]. Our main interest is to outline how A & P compute the Čech cohomology with integer coefficients of the tiling space $H^i(\Delta, \mathbb{Z})$ for $i \in \mathbb{N}_0$. For an overview of Čech cohomology for tiling spaces and other versions of tiling cohomology, see [BK10].

Proposition 3.12. *If the substitution tiling forces its border then $H^i(\Delta, \mathbb{Z})$ is isomorphic to the direct limit of the system of abelian groups*

$$H^i(\Gamma_0, \mathbb{Z}) \xrightarrow[\gamma_0^*]{} H^i(\Gamma_0, \mathbb{Z}) \xrightarrow[\gamma_0^*]{} \cdots$$

for $i = \mathbb{N}_0$.

For a proof of Proposition 3.12 see [AP98, Theorem 6.1]. Since $\varprojlim \Gamma_0 = \Delta_0$ and Δ_0 is homeomorphic to Δ, the following are all isomorphic:

$$H^i(\Delta, \mathbb{Z}) \cong H^i(\Delta_0, \mathbb{Z}) = H^i(\varprojlim \Gamma_0, \mathbb{Z}) \cong \varinjlim H^i(\Gamma_0, \mathbb{Z}).$$

The computation of the direct limit of abelian groups $\varinjlim H^i(\Gamma_0, \mathbb{Z})$ is accessible. For $0 \leq i \leq M$ let c_i denote the number of cells c_i of dimension i in the CW-complex Γ_0. In the cellular cohomology complex for Γ_0, the group of cochains in dimension i are identified with $\mathbb{Z}^{c_i}$. The cellular map γ_0 induces a map on cochains which in dimension i is associated with a $c_i \times c_i$ integer matrix denoted A'_i. For $i = M$, the top dimension, the matrix A'_M is exactly the transpose of the $c_M \times c_M$ matrix $A_{(jk)}$ whose entries indicate how many times the cell j occurs in the inflation of cell k. The maps $\delta'_i : \mathbb{Z}^{c_{i-1}} \to \mathbb{Z}^{c_i}$ are the usual boundary maps.

Example 3.13. Summarising results in [AP98], for the golden-b substitution IFS the corresponding cell complex Γ_0 has eight faces, eight edges, and three vertices: $\bar{F} = \{A, B, C, D, E, F, G, H\}$, $\bar{E} = \{a, b, c, d, e, f, g, h\}$, $\bar{V} = \{\alpha, \beta, \gamma\}$. So $\delta'_1 : \mathbb{Z}^{|\bar{V}|} \to \mathbb{Z}^{|\bar{E}|}$ is an 8×3 matrix indicating the initial and final vertices for the edges and $\delta'_2 : \mathbb{Z}^{|\bar{E}|} \to \mathbb{Z}^{|\bar{F}|}$ is an 8×8 matrix indicating the edges (with orientation) that surround the perimeter of each face. The matrices A'_0, A'_1 and A'_2 indicate how the vertices, edges and faces are respectively subdivided under the inflation map (see [AP98] for the full matrices). We remind the reader that Figure 3.2 displays example subdivisions for faces A and E. The rank of these matrices are

$$\mathrm{rank}(\delta'_2) = 2,\ \mathrm{rank}(\delta'_1) = 2,\ \mathrm{rank}(A'_2) = 8,\ \mathrm{rank}(A'_1) = 8,\ \mathrm{rank}(A'_0) = 3.$$

From these ranks and Proposition 3.12 it follows that

$$H^0(\Delta) \cong \mathbb{Z},\ H^1(\Delta) \cong \mathbb{Z}^4,\ H^2(\Delta) \cong \mathbb{Z}^6.$$

3.3 Collared Tiles

Forces its border turns out to be quite a strong requirement. Many interesting examples, such as the Fibonacci IFS, do not have this property.

Example 3.14. Let $(\mathcal{F}, \mathcal{G})$ be the Fibonacci IFS from section 1.4.1. The corresponding substitution IFS has two vertices which we label $\{a, b\}$ and three maps

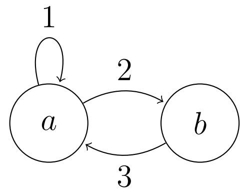

Figure 3.4: Substitution Fibonacci graph

(see the graph in Figure 3.4). This presentation matches the representation of the Fibonacci substitution as a system with two rules: $a \to ab$ and $b \to a$. So we think of the inflation map ω as taking the tile a to tiles ab and the tile b to a tile a. Let T and T' be two Fibonacci tilings such that T contains the string baa and T' contains the string aab. Considering inflations of the string $\omega^M(aab)$, we observe that $\omega^M(\{a\})$ is neighboured by b on the left and a on the right when M is odd and a on both sides when M is even. In contrast, for inflations of the string $\omega^M(baa)$, $\omega^M(\{a\})$ is neighboured by b on the left and a on the right when M is even and a on both sides when M is odd. So there will never exist an M such that $\omega^M(\{a\})$ coincides on all the neighbouring tiles.

If the tiling does not force its border the map from Δ to Δ_0 in Proposition 3.11 is still well-defined but fails to be injective. Hence, another key idea of A & P was to build a new complex made from tiles together with labels indicating the pattern of neighbouring tiles (called collared tiles).

Definition 3.15. Let t be a tile in $T \in \Delta$, then $T^1(t) = \{t' \in T : t' \cap t \neq \emptyset\}$ is the collared tile in T containing t.

Definition 3.16. Define

- $\Gamma_1 = \Delta \times \mathbb{R}^d / \sim_1$ as the product space with the equivalence $(T_1, u_1) \sim_1 (T_2, u_2)$ if tiles t_1 and t_2 with $u_1 \in t_1$ and $u_2 \in t_2$, satisfy $T_1^1(t_1) - u_1 = T_2^1(t_2) - u_2$,

- $(T, u)_1$ as the equivalence class of a point (T, u),

- $\gamma_1 : \Gamma_1 \to \Gamma_1$ as the continuous map induced by ω and defined by $\gamma_1((T, u)_1) = (\omega(T), \lambda u)_1$,

- $\Delta_1 = \varprojlim \Gamma_1$ and a right shift map $\omega_1 : \Delta_1 \to \Delta_1$ by $\omega_1(x)_i = \gamma_1(x_i)$.

A & P show that (Δ_1, ω_1) is always topologically conjugate to (Δ, ω) and if the substitution forces its border, then (Δ_1, ω_1) is topologically conjugate to (Δ_0, ω_0) (see [AP98, Theorem 4.3]). Hence, for any substitution tiling, $H^i(\Delta, \mathbb{Z})$ is isomorphic to the direct limit $\varinjlim H^i(\Gamma_1, \mathbb{Z})$ (again see [AP98, Theorem 6.1]).

Example 3.17. Returning to the Fibonacci example (again summarising results from [AP98]), it is clear from inspection that there are only four strings of length three that can occur in any tiling. These correspond to the four collared tiles $\{aab, baa, bab, aba\}$, which we label as $\{c, d, e, f\}$ respectively. We subdivide these tiles by applying γ_1. Slightly abusing notation, we write $\gamma_1(c) = (ab\underline{ab}a) = ef$ where $ab\underline{ab}a$ is the expansion of the string $c = aab$ by the usual inflation. We underline the substring $\underline{ab}$ to emphasise that this is the expansion of the prototile a. We find the collared tiles in the inflation by determining which strings of length three are contained in the set of tiles made from $\omega^N(\{a\})$ and its immediate neighbours:

$$\begin{aligned}
\gamma_1(c) &= (ab\underline{ab}a) = ef \\
\gamma_1(d) &= (a\underline{ab}ab) = cf \\
\gamma_1(e) &= (a\underline{ab}a) = cf \\
\gamma_1(f) &= (ab\underline{a}ab) = d.
\end{aligned}$$

The complex Γ_1 is made with three vertices $\{u, v, w\}$ and the four edges $\{c, d, e, f\}$,

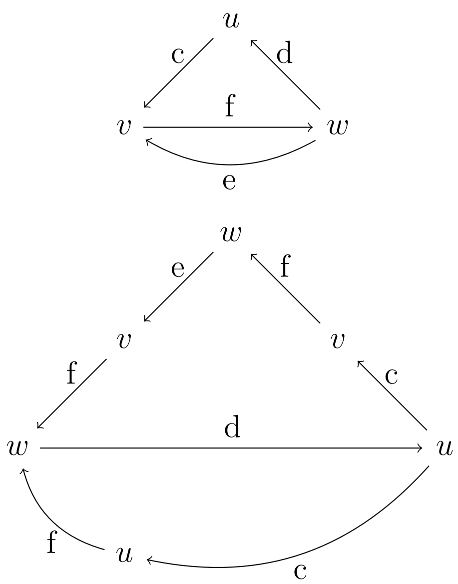

Figure 3.5: Collared Fibonacci cell complex before and after inflation

as pictured at the top of Figure 3.5. Below, we display the cell complex after inflation. From this figure, we can read off the values for δ_1', A_1' and A_0'. These matrices are

$$\delta_1' = \begin{bmatrix} -1 & 1 & 0 \\ 1 & 0 & -1 \\ 0 & 1 & -1 \\ 0 & -1 & 1 \end{bmatrix} \quad A_1' = \begin{bmatrix} 0 & 0 & 1 & 1 \\ 1 & 0 & 0 & 1 \\ 1 & 0 & 0 & 1 \\ 0 & 1 & 0 & 0 \end{bmatrix} \quad A_0' = \begin{bmatrix} 0 & 0 & 1 \\ 0 & 0 & 1 \\ 1 & 0 & 0 \end{bmatrix}$$

with $\mathrm{rank}(\delta_1') = 2$, $\mathrm{rank}(A_1') = 3$, $\mathrm{rank}(A_0') = 2$. Calculating yields

$$H^0(\Delta) \cong \mathbb{Z}, H^1(\Delta) \cong \mathbb{Z}^2.$$

Remark 3.18. For the IFS setting, switching to collared tiles generates a new IFS. The collared Fibonacci IFS has seven maps $\mathcal{F}_c = \{f_1, ...f_7\}$ and graph with vertex set $\{C, D, E, F\}$ corresponding to the four prototiles displayed in Figure 3.6. All the maps have the same scaling factor. Also note that this new IFS is not locally rigid, but importantly it does force its borders. By A & P's result this means it can be used to calculate the cohomology of the original tiling space.

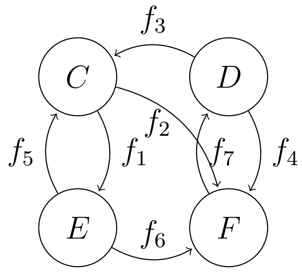

Figure 3.6: Collared Fibonacci IFS graph

Chapter 4

Neighbour Graphs

While chapter 3 links the tiling IFS framework to A & P theory, this chapter connects the framework to the study of neighbour graphs in fractal geometry. Both of these connections to the literature are expanded upon in chapter 5 in the discussion of mixed tiling systems.

For the entirety of this chapter, we restrict our attention to iterated function systems where the graph has one sole vertex. So for an IFS of the form $\mathcal{F} = \{\mathbb{R}^M; f_1, f_2, ...f_N\}$, the full address space is $[N]^* \cup [N]^\infty$. Letting A denote the attractor of some IFS, we set $A_i := f_i(A)$ for $i \in [N]^*$. Considering two strings $j, k \in [N]^*$, we can ask whether the corresponding subsets A_j and A_k intersect. They could intersect at a point, a countable set, an uncountable set, or be entirely disjoint. Studying neighbouring pieces and their corresponding maps has been a long interest of Bandt and various collaborators. They show in [BG92, BHR05, BM09] how the neighbour map theory allows one to check the 'open set condition' (defined in 4.1), describe properties of the fractal including connectness and boundary dimensions, and view the fractal as the quotient of a symbolic space.

Section 4.1 introduces the neighbour map theory, with a particular emphasis on showcasing an interesting example from [BM18]. As far as we know, the theory is only thoroughly developed for systems whose maps have uniform scaling factors. In section 4.2, we propose an extension of the theory to cover the case when the IFS maps have scalings that are integer powers of some $0 < s < 1$. From this extension, we can apply the neighbour map theory to study a wider range of tiling IFSs. The Sierpinski, rigid Williams, Fibonacci, and golden-b all make appearances.

4.1 Uniform Scaling

To introduce neighbour maps and graphs, we consider an IFS $\mathcal{F} = \{\mathbb{R}^M; f_1, f_2, ...f_N\}$, where each f_i is an invertible contractive similitude with scaling factor $0 < s < 1$. In this setting, neighbouring pieces to the attractor A are always isometric to A itself.

Take strings $i, j \in [N]^*$ such that $|i| = |j|$ and consider maps of the form $h = f_i^{-1} f_j$. The map h takes A onto its potential neighbour $h(A)$, which has the same position with respect to A as A_j does with A_i. The map $h = f_i^{-1} f_j$ is called a proper neighbour map if $A_i \cap A_j \neq \emptyset$. These neighbour map are generated recursively. Starting with maps of the form $h_1 = f_{i_1}^{-1} f_{j_1}$ with $i_1 \neq j_1 \in [N]$, we find further maps by setting $h_2 = f_{i_2}^{-1} h_1 f_{j_2}$ for $i_2, j_2 \in [N]$. This process continues, and in fact all neighbour maps are obtained by applying the interior automorphism $\Phi_{ij}(h) = f_{i_1}^{-1} h f_{j_1}$ for $i, j \in [N]$ starting with $h = id$ [BM09].

Definition 4.1. For the uniform scaling setting, define the set of proper neighbours as

$$\mathcal{N} = \{f_i^{-1} f_j : i, j \in [N]^*, |i| = |j|, f_i(A) \cap f_j(A) \neq \emptyset\}.$$

The neighbour graph is constructed by setting the vertex set to be the set of proper neighbour maps. There is a directed edge, labelled (i, j), from vertex h to vertex $\bar{h}$ if $\bar{h} = f_i^{-1} h f_j$ for some $i, j \in [N]$. The identity map id denotes the root vertex of the graph but by convention it is not included in the figures and all edges from the root have no initial vertex. An IFS $\mathcal{F}$ is said to be of finite type if there are only finitely many proper neighbour maps and hence only finitely many vertices in the neighbour graph [BM09].

For $(j, k) \in [N]^*$ the set $f_j^{-1} f_k(A)$ is called a neighbour of A and $f_j^{-1} f_k$ referred to as the corresponding neighbour map. The intersection $f_j^{-1} f_k(A) \cap A$ of the fractal A with its neighbour is called an edge of A.

Definition 4.2. An IFS $\mathcal{F} = \{\mathbb{R}^M; f_1, f_2, ...f_N\}$ is said to satisfy the open set condition (OSC) if there exists a nonempty open set $V \subset \mathbb{R}^M$ such that

$$\bigcup_{i=1}^{N} f_i(V) \subseteq V \text{ and } f_i(V) \cap f_j(V) = \emptyset \text{ for } i \neq j.$$

From the neighbour graph, the OSC can be checked. Bandt and Graf proved that the OSC is equivalent to the condition that neighbour maps cannot converge to the identity [BG92]. When the $\mathcal{F}$ is of finite type, this is equivalent to requiring that there is no map back to the id vertex in the neighbour graph.

Example 4.3. To get a feel for how to construct neighbour graphs, we begin by considering the Sierpinski IFS, $\mathcal{F} = \{f_1, f_2, f_3\}$, defined in section 2.3.1. Though we have not seen this neighbour graph presented explicitly before, for anyone familiar with neighbour map theory it would be an easy computation. To find the set of proper neighbours, we consider the ways an isometric copy of the attractor A can intersect $\Pi(\emptyset)$. With $\Pi(\emptyset)$ shaded in red, Figure 4.1 shows that there are six ways, corresponding to the existence of six proper neighbour maps. The complete set of non-trivial neighbour maps for the Sierpinski IFS is

$$\mathcal{N} = \{f_1^{-1}f_2, f_2^{-1}f_1, f_1^{-1}f_3, f_3^{-1}f_1, f_2^{-1}f_3, f_3^{-1}f_2\}.$$

So the neighbour graph has six vertices which we label as $r = f_1^{-1}f_2$, $r^- = f_2^{-1}f_1$,

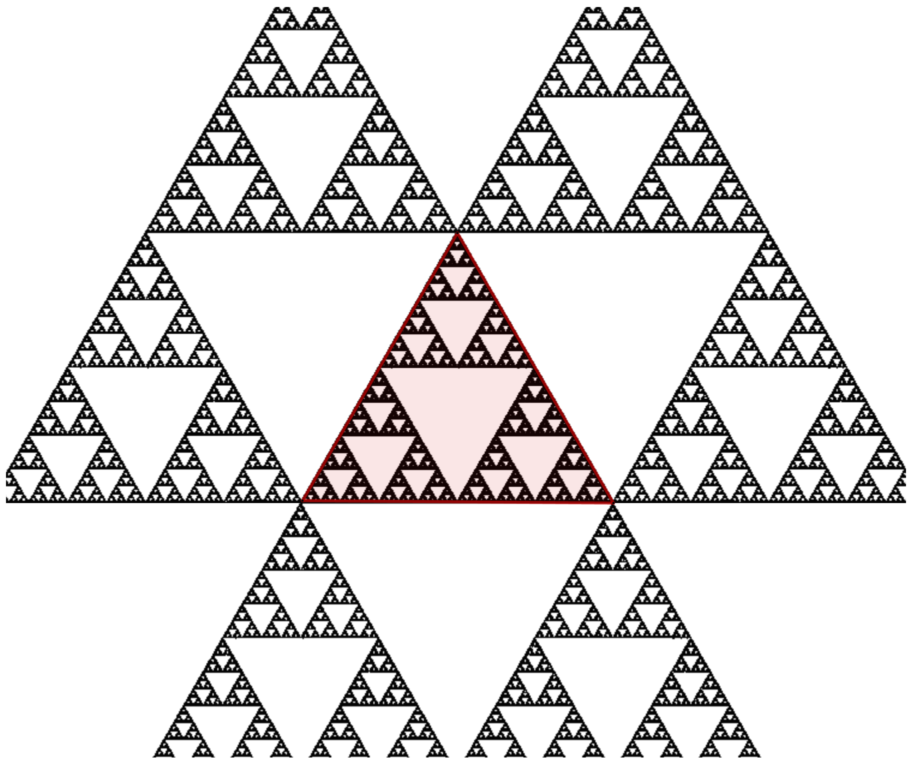

Figure 4.1: Sierpinski neighbours

$s = f_1^{-1}f_3$, $s^- = f_3^{-1}f_1$, $t = f_2^{-1}f_3$, and $t^- = f_3^{-1}f_2$. The pairs (A_j, A_k) for $j \neq k$ intersect on a point, so there is only one subpiece $(A_{jj'}, A_{kk'})$ for some pair $(j', k') \in [3] \times [3]$ such that $A_{jj'} \cap A_{kk'} \neq \emptyset$.

Consider the neighbour map $r = f_1^{-1}f_2$ which maps A_1 to A_2. We observe that $A_{12} \cap A_{21} \neq \emptyset$. How does A_{12} map to A_{21}? Exactly by applying the map r, which algebraically is justified by the equality $f_2^{-1}(f_1^{-1}f_2)f_1 = f_1^{-1}f_2$ for these explicit functions. So we have a loop labelled $(2,1)$ on r in the neighbour graph. We find such loops for all the other vertices, yielding the full neighbour graph as displayed in Figure 4.2.

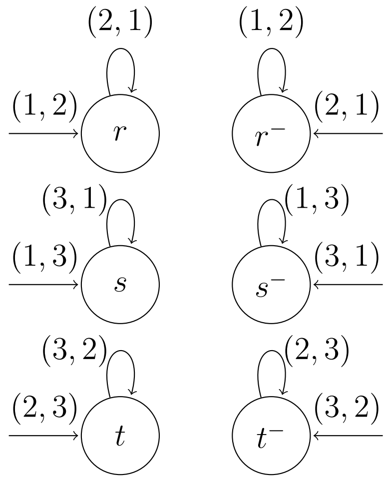

Figure 4.2: Sierpinski neighbour graph

It is well known that the symbolic space quotiented out by the set of equivalent addresses is homeomorphic to the attractor itself. Let $r \sim t$ if $\pi(r) = \pi(t)$, then $\pi : \frac{[N]^\infty}{\sim} \to A$ is a homeomorphism [Bar93]. Recall that the coding map from Theorem 1.12 is surjective but not generally injective. In [BM09] Bandt and Mesing state that "pairs of equivalent addresses coincide with labelled sequences of infinite edge paths in the neighbour graph". Their proof is short and we believe a more thorough and explicit justification of this equivalence is clarifying.

Proposition 4.4. *The following is true: $\pi(r) = \pi(t)$ if and only if for some $n \in \mathbb{N}$, $r_1...r_{n-1} = t_1...t_{n-1}$ and $h = f_{r_n}^{-1} f_{t_n}$ is a proper neighbour map with an arrow to it from the identity vertex and $(S^n(r), S^n(t))$ coincides with a sequence of infinite edge paths starting from h in the neighbour graph.*

Proof. The backwards direction is easy. Assuming $r_1...r_{n-1} = t_1...t_{n-1}$ and $h = f_{r_n}^{-1} f_{t_n}$ is a proper neighbour map means that $A_{r_1...r_n} \cap A_{t_1...t_n} \neq \emptyset$. Then following an infinite edge of paths from this vertex implies that $A_r \cap A_t \neq \emptyset$, so $\pi(r) = \pi(t)$.

For the forward direction, supposing $r \neq t \in [N]^\infty$ with $\pi(r) = \pi(t)$ gives us that $A_r \cap A_t \neq \emptyset$. The points A_r and A_t either lie in a single copy A_i or on the boundary of multiple sets A_i for $i \in \{1, 2...N\}$. If they lie in a single copy A_{i_1}, then set $r_1 = t_1 = i_1$. Next, consider the sets of the form $A_{i_1 j}$ and check for $j \in \{1, 2...N\}$ whether the points A_r, A_t lie in one or multiple sets. We continue until the points eventually lie on the intersection of at least two sets. Say this is at stage $n \in \mathbb{N}$, then label two of the different indices of the sets that the points are bordering as $k \neq l \in \{1, 2...N\}$. We set $r_n = k$ and $t_n = l$ and observe that $h = f_{r_1...r_n}^{-1} f_{t_1...t_n} = f_{r_n}^{-1} f_{t_n}$ is a proper neighbour map which has an arrow to it from the identity vertex in the neighbour graph. Since $\pi(r) = \pi(t)$, from vertex h there is an infinite path in the graph $(S^n(r), S^n(t))$ that corresponds to the tail of strings r and t. $\square$

This proposition says that a purely symbolic description of the attractor can be obtained from the neighbour graph. From the graph, we can determine all the equivalent addresses of points on the attractor. By Example 4.3 and Proposition 4.4, all equivalent addresses in the Sierpinski attractor end in pairs $(1\bar{2}, 2\bar{1}), (1\bar{3}, 3\bar{1})$ or $(2\bar{3}, 3\bar{2})$.

Now, we shift our focus to recent work by Bandt and Mekhontsev who recently discovered some new relatives of the Sierpinski gasket [BM18]. The IFSs for these relatives are all generated by three maps:

$$f_k(z) = \frac{1}{2} s_k(z + c_k) \text{ for } k = 0, 1, 2$$

where $c_k = a_k + ib_k$ with $a_k, b_k \in \mathbb{Z}$, the points $\{c_0, c_1, c_2\}$ are non-collinear, and $s_k \in \{id, s(z) = iz, s^2(z) = -z, s^3(z) = -iz\}$. So the maps are integer translations with a rotation around $0, \pm 90°$ or $180°$ with scaling factors $\frac{1}{2}$. Additionally, they require that the IFS satisfies the open set condition. The Hausdorff dimension of all these relatives' attractors is $\frac{\log(3)}{\log(2)} \approx 1.585$. Alongside showcasing some well known examples including the Sierpinski triangle and the two dimensional Cantor set, they present some new examples that satisfy these constraints. The simplest new example they describe is called 'Crossings'. This example nicely demonstrates how the neighbour graph can be used to compute properties of the fractal including connectedness and boundary dimension. All the results and computations for this example follow [BM18].

Example 4.5. Let $\mathcal{F} = \{f_0(z) = \frac{-iz}{2}, f_1(z) = \frac{-1}{2}(z - 1 - i), f_2(z) = \frac{-1}{2}(z + 1)\}$ be the Crossings IFS with attractor A displayed in Figure 4.3. We observe from Figure 4.3 that A_1 and A_2 differ by a translation. Let $t = f_1^{-1} f_2$ be the translation taking A_1 to A_2 computed as $t(z) = z - 2 - i$. Let $t^- = f_2^{-1} f_1$ be the inverse which translates A_2 to A_1 by $t^-(z) = z + 2 + i$. Note that $A_{12} \cap A_{21} \neq \emptyset$ and A_{12} is mapped to A_{21} by t^- since there is a $180°$ rotation in the maps f_1 and f_2. Algebraically, we check that $f_2^{-1}(f_1^{-1} f_2) f_1 = f_2^{-1} f_1$. This means, in the neighbour

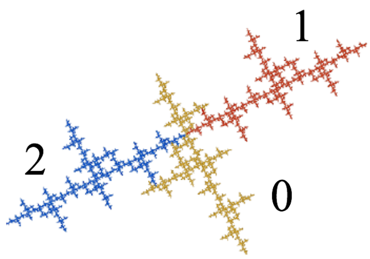

Figure 4.3: Crossings attractor [BM18]

graph, there is an edge labelled $(1, 2)$ from t to t^- and by a similar computation there is another edge $(2, 1)$ from t^- to t.

Other neighbour maps are $r = f_0^{-1} f_1$ and $u = f_0^{-1} f_2$ and their inverse. Going a level deeper, we find that A_{00} maps to A_{11} by the map $s(z) = -z + 1$ which is self-inverse; $s = s^-$. It turns out that these seven maps are all the possible neighbours. The set

$$\mathcal{N} = \{t, t^-, r, r^-, u, u^-, s\},$$

see Figure 4.4, is complete since for any $h \in \mathcal{N}$ and any pair $j, k \in \{0, 1, 2\}$ the map $\bar{h} = f_j^{-1} h f_k$ is also in $\mathcal{N}$. By the same methods as before, we find the edges between the vertices and complete the neighbour graph (displayed in Figure 4.5).

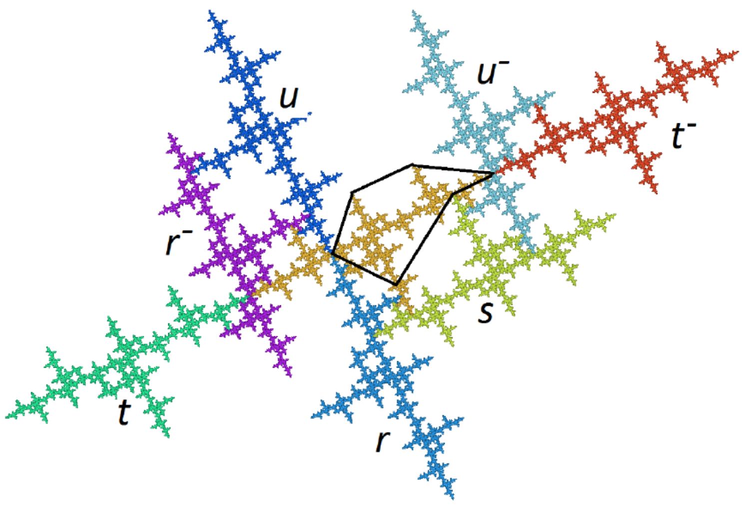

Figure 4.4: Crossing neighbours [BM18]

Since $\mathcal{F}$ has finite type and there is no map in the neighbour graph back to the identity, the crossing IFS satisfies the OSC. From the neighbour graph, we

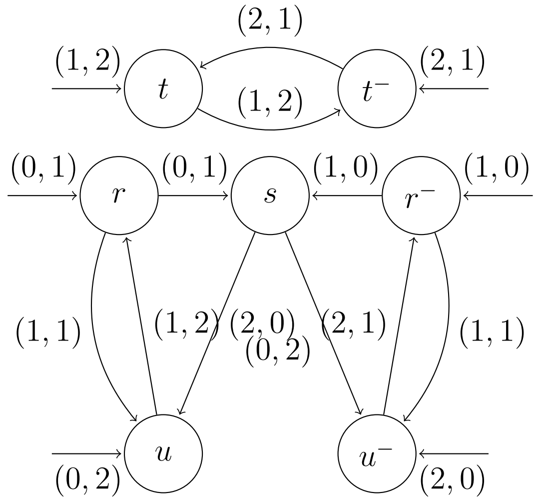

Figure 4.5: Crossings neighbour graph

can read off that $1\bar{12}$ and $2\bar{21}$ are equivalent addresses corresponding to the single point of intersection between A_1 and A_2. We also observe the lower connected portion of the Crossing neighbour graphs has several cycles with a common vertex. By [BM09], $A_0 \cap A_1$ and $A_0 \cap A_2$ are Cantor sets.

The edge corresponding to a neighbour map is denoted by the capitalisation of the map's label. For example, the corresponding edge for the map $r = f_0^{-1} f_1$ is denoted by $R = r(A) \cap A$. We know from above that R is a Cantor set but it turns out that from the neighbour graph its dimension can be computed explicitly. The edges themselves are self-similar, made from copies of other edges with one of the maps f_0, f_1, f_2 applied. Since two edges from vertex r are directed to vertices u and s, the edge R is made from self-similar copies of the edges U and S. The vertex u has only one outgoing edge, labelled 1 directed to r. The vertex s has an edge labelled 2 to u and 0 to u^-. This yields the equations

$$R = f_1(U) \cup f_0(S), U = f_1(R), S = f_2(U) \cup f_0(U^-).$$

The edge U^- is isometric to U by an isometry we label u^-. Then

$$\begin{aligned} R &= f_1 f_1(R) \cup f_0(f_2(U) \cup f_0(U^-)) \\ &= f_1^2(R) \cup f_0 f_2 f_1(R) \cup f_0 f_0 u^- f_1(R) \end{aligned}$$

So R is a self-similar set that is the union of maps with scaling factors $\{\frac{1}{4}, \frac{1}{8}, \frac{1}{8}\}$. The Hausdorff dimension α for a self-similar set is computed in the usual way as the solution to

$$(\frac{1}{4})^\alpha + 2(\frac{1}{8})^\alpha = 1.$$

Rearranging and letting $y = 2^\alpha$ we solve $y + 2 = y^3$, finding $y \approx 1.521$ and hence $\alpha \approx 0.6054$ is the approximate Hausdorff dimension. Similar arrangements and calculations show that $\alpha \approx 0.6054$ is the dimension of edges U and S as well.

4.2 Integer Power Scaling

We consider neighbour maps and graphs for the more general setting where the scaling factors of the maps in the IFS are integer powers of some fixed ratio. This more closely links the tiling IFS story to the neighbour theory since we require the same algebraic condition on the IFS maps in Definition 1.13.

Definition 4.6. For an IFS $\mathcal{F} = \{f_1, \dots f_N\}$ with fixed $0 < s < 1$ and scaling factors s^{a_i} for $i \in \{1, \dots N\}$, we define the set of neighbour maps to be

$$\mathcal{N} = \{f_i^{-1} f_j : i, j \in [N]^*, \text{ neither } i \sqsubseteq j \text{ nor } j \sqsubseteq i, |\xi(i) - \xi(j)| < a_{\max}\},$$

where for $k, l \in [N]^*$, $k \sqsubseteq l$ denotes that k is a prefix of l.

The condition on the difference between the total scaling of the strings ensures that the neighbour map takes A to a similar copy $f_i^{-1} f_j(A)$ which is isometric to something in the set $\{s^{\pm n} A\}$ for $n \in \{0, 1, ..., a_{\max} - 1\}$. From the tiling perspective, this requirement means that the attractor copies A_i and A_j are possible neighbouring tiles in an expanded tiling made from the map Π.

We can generate a subset of the neighbour maps recursively. These neighbours correspond exactly to the vertices in the neighbour graph that are reached by a directed path from the identity vertex.

Definition 4.7. We define a set of symbolic neighbour pairs as

$$P = \{(i, j) \in [N]^* \times [N]^* : \xi(i), \xi(j) \leq a_{\max}\}.$$

Starting with a map $h_1 = f_i^{-1} f_j$ such that $(i, j) \in P$ with $i_1 \neq j_1$, we find further maps by considering the possible pairs $(i', j') \in P$ such that $|\xi(ii') - \xi(jj')| < a_{\max}$. Then $h_2 = f_{ii'}^{-1} f_{jj'}$ is another neighbour map. We continue this way generating maps of the form $h_n = f_{ii'...i^{(n)}}^{-1} f_{jj'...j^{(n)}}$ for any $n \in N$ with each pair $(i^{(k)}, j^{(k)}) \in P$ for $1 \leq k \leq n$ and $|\xi(ii'...i^{(n)}) - \xi(jj'...j^{(n)})| < a_{\max}$.

Let $h \in \mathcal{N}$ be a proper neighbour if $A \cap h(A) \neq \emptyset$. As in the simplified setting, we set the neighbour graph's vertex set to be exactly the set of proper neighbour maps. There is a directed edge in the graph from $h \in \mathcal{N}$ to $\bar{h} \in \mathcal{N}$, labelled by $(i, j) \in P$, if $\bar{h} = f_i^{-1} h f_j$. We only keep the arrows that correspond to proper neighbours. Again, we say that A is of finite type if there are only finitely many proper neighbour maps and in such cases there will only be finitely many vertices in the graph. We illustrate these ideas for the rigid Williams.

Example 4.8. Let $\mathcal{F} = \{\mathbb{R}^2; f_1, f_2, f_3\}$ be the rigid Williams IFS defined explicitly in section 2.3.2 with attractor $A \subset \mathbb{H}(\mathbb{R}^2)$. The set of symbolic neighbour pairs is

$$P = \{(i, j) : i, j \in \{1, 2, 3, 11\}\}.$$

To find the proper neighbour maps that can be reached from the identity vertex in the neighbour graph, we consider all maps of the form $f_i^{-1} f_j(A) \cap A \neq \emptyset$ for $(i, j) \in P$ with $i_1 \neq j_1$. By inspection it is clear that $r = f_3^{-1} f_2$, $p = f_2^{-1} f_1$, $t = f_3^{-1} f_1$ and their inverses are the only such maps. The map r corresponds to a flip, rotation, and translation (no scaling). The map p is a rotation and expansion (no flip) and the map t is a flip, rotation, expansion and translation. These three maps, along with all the other neighbour maps, are displayed in Figure 4.6. In Figure 4.6, the tail of arrow indicates which set is viewed as the attractor and the head indicates the attractor's neighbour for that map.

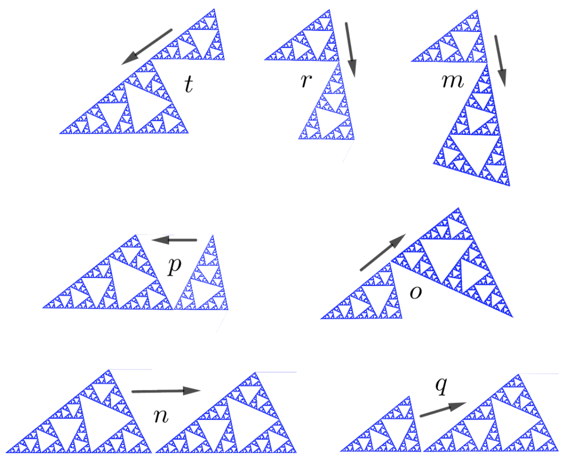

Figure 4.6: Rigid Williams neighbours

Since the sets A_1, A_2 and A_3 intersect on at most a point, it is not difficult to determine how their subpieces are mapped to one another. Starting with neighbour map r, both $q = f_2^{-1} r f_1$ and $g = f_2^1 r f_{11}$ intersect to give new proper neighbours. The map q is a flip, rotation, expansion while the map n is simply a translation.

The pair $(3,3)$ is the only element in P that gives a proper neighbour from p. In fact, the subpiece A_{23} is mapped to A_{13} by applying the map p. This corresponds to a loop $(3,3)$ in the neighbour graph in Figure 4.7.

The pair $(1,2)$ is the only element in P that gives a proper neighbour from t. The subpiece A_{31} is mapped to A_{12} by applying r^-. There is a directed edge labelled $(1,2)$ from t to r^-. Going one level deeper we find another proper neighbour $m = f_2^{-1} n f_1$. This map is a flip, rotate, expand and translation.

So far we have twelve vertices: m, n, p, q, r, t and their inverses. Let h be any of these vertices. We find all the edges from these vertices in the neighbour graph by checking for which pairs $(i,j) \in P$, $f_i(A) \cap h(f_j(A)) \neq \emptyset$. From these calculations we complete the component of the neighbour graph connected to the identity vertex.

However, we observe that there is another neighbour map that cannot be reached from the identity. Consider the mapping between the subpiece A_{113} and A_{12}. Let $o = f_{113}^{-1} f_{12} \in \mathcal{N}$ which is a rotation and expansion (no flip, no translation). The subpiece A_{1133} is mapped to A_{123} by applying the map o. Just like the case for vertex p, this corresponds to a loop $(3,3)$ in the neighbour graph in Figure 4.7.

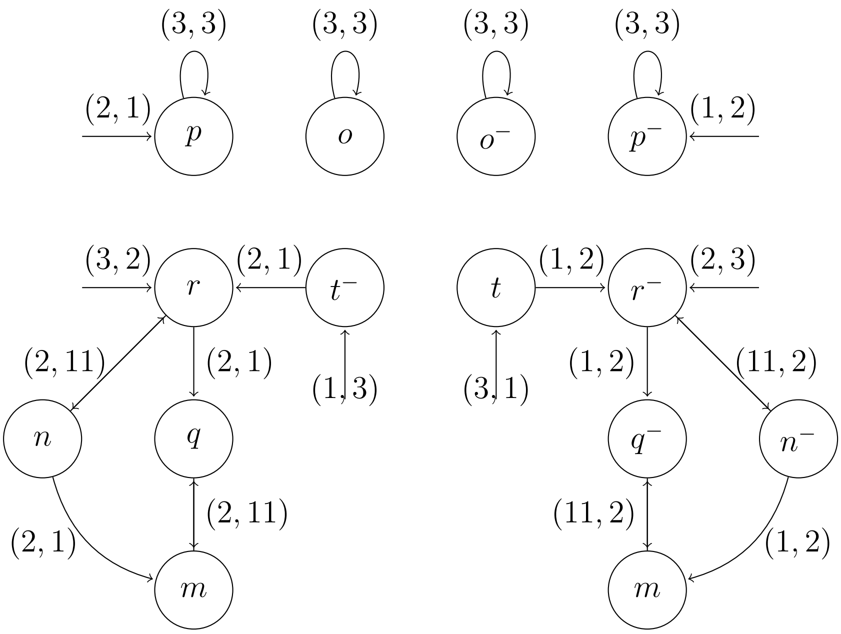

Figure 4.7: Rigid Williams neighbour graph

We believe that there are no more neighbour maps and that some geometric argument with angles could verify this but we have not included such an argument in this thesis. For our current purposes, the full neighbour graph is taken to be the one displayed in Figure 4.7.

Inspecting the rigid Williams' neighbour graph, we observe that there are eight pairs of infinite edge paths: $p_1 = (3\bar{2}, 2\bar{1}), p_2 = (2\bar{3}, 1\bar{3}), p_3 = (3\bar{1}, 1\bar{2}), p_4 = (113\bar{3}, 12\bar{3})$ and their inverses. Note that we can equivalently express the fourth pair as

$$\begin{aligned} p_4 &= (11\bar{3}, 12\bar{3}) \\ &= (1,1) + (1\bar{3}, 2\bar{3}) \\ &= (1,1) + p_2^- \end{aligned}$$

where $+$ is the concatenation of strings. The pair p_4 was identified from a vertex not connected to the identity component of the neighbour graph. As expected by Proposition 4.4, we can express this infinite path as a pair (r,t) such that $r_1 = t_1$ and $h = f_{r_2}^{-1} f_{t_2} = f_1^{-1} f_2$ is a proper neighbour map that has an arrow to it from the identity vertex and $(S^2(r), S^2(t)) = Sp_2^-$ coincides with an infinite path in the neighbour graph from vertex h.

Remark 4.9. There is still work to be done to properly check this proposed extension to the neighbour graph theory. However, the rigid Williams computation gives hope that the construction is reasonable and provides interesting information about the fractal attractor and tiling IFS.

To inspect whether this extension seems sensible on more examples, and also not wanting our other key characters to feel left out in this chapter, we compute the Fibonacci neighbour graph and begin the computation for the golden-b neighbour graph.

Example 4.10. Recall from section 1.4.1 that the Fibonacci IFS has two maps $\{f_1, f_2\}$ with scaling factors s and s^2 respectively. The set of symbolic neighbour pairs is $P = \{(i,j) : i,j \in \{1,2,11\}\}$. The only maps of the form $f_i^{-1} f_j$ such that $f_i(A) \cap f_j(A) \neq \emptyset$ for $(i,j) \in P$ with $i_1 \neq j_1$ are $t = f_1^{-1} f_2$ and $t^- = f_2^{-1} f_1$. These correspond to the two vertices that can be reached from the identity. Since $f_2^{-1} t f_{11} = t$ there is a loop on t labelled $(2, 11)$. The subpieces A_{12} and A_{21} intersect and give another neighbour map $r = (f_{12})^{-1} f_{21}$. There is a directed edge from t to r labelled $(2,1)$ since $r = f_2^{-1} t f_1$. Also, $f_2^{-1} r f_{11} = r$ so there is a loop on r labelled $(2, 11)$. We find another neighbour $s = f_2^{-1} r f_1$ which has a directed edge going to it from r labelled $(2,1)$. There is also a loop on s labelled

$(2, 11)$. Similar computations find the edges between neighbours t^-, r^-, s^-. The complete neighbour graph is displayed in Figure 4.8. The graph tells us that equivalent addresses must end in strings $1\bar{2}$ and $2\bar{1}$ as we would expect.

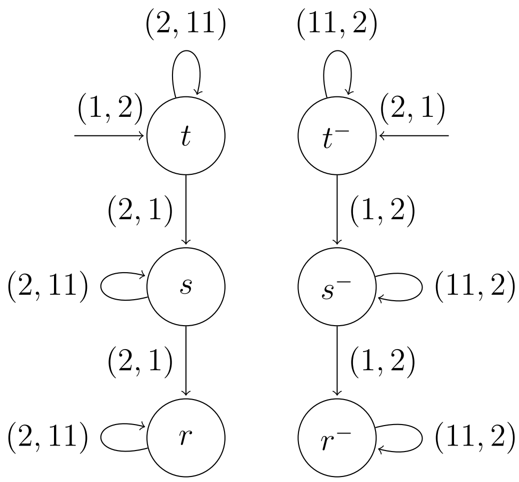

Figure 4.8: Fibonacci neighbour graph

Example 4.11. The golden-b IFS consists of two maps $\{f_1, f_2\}$, attractor $G \subset \mathbb{R}^2$ and prototile set $\{S, L\}$. The set of symbolic neighbour pairs matches that for the Fibonacci IFS: $P = \{(i, j) : i, j \in \{1, 2, 11\}\}$. The maps of the form $f_i^{-1} f_j$ such that $f_i(G) \cap f_j(G) \neq \emptyset$ for $(i, j) \in P$ with $i_1 \neq j_1$ are $v = f_1^{-1} f_2$, $v^- = f_2^{-1} f_1$, $w = f_{11}^{-1} f_2$ and $w^- = f_2^{-1} f_{11}$. Focussing on $v = f_1^{-1} f_2$ as a vertex in the graph, we find five directed edges $\{e_1, ...e_5\}$ from v that connect to five other vertices $\{w_1, ...w_5\}$. These five vertices correspond to five other neighbour maps pictured in Figure 4.9. Two pairs in P that do not correspond to an edge from v are $(1, 2)$ and $(2, 1)$. This is because $f_{12}^{-1}(G) \cap f_{21}(G) = \emptyset$ and $|\xi(22) - \xi(11)| = 2$. The full neighbour graph for the golden-b is very large since there are many ways two tiles in a golden-b tiling can intersect.

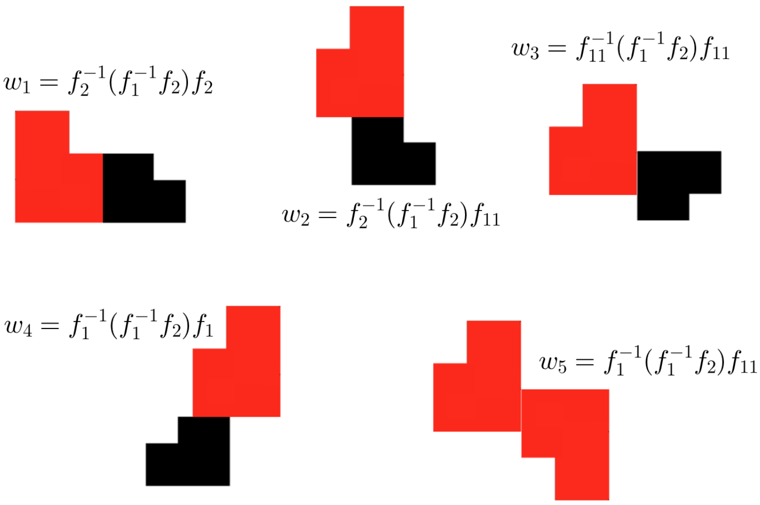

Figure 4.9: Some golden-b neighbours

Chapter 5

Mixed Tilings Systems

This chapter is motivated by the idea that having a nice family of tiling IFSs allows us to define a notion of mixed tiling systems and obtain an interesting variety of tilings. The general idea of mixed systems has appeared in numerous places within recent tiling and fractals literature. Gahler and Maloney's 2013 paper investigate the cohomology of one-dimensional mixed substitution tiling spaces [GM13]. Bandt, Mekhontsev and Tetenov, in their recent 2018 paper, provide an example tiling with fractal boundary pieces that has the same symmetry and spectral properties as the pinwheel triangle [BMT18]. In the paper, two possible IFSs for the fractal pinwheel tiling are provided which we recognised as a two-dimensional example for the mixed tiling theory.

In section 5.1, we set up the notation and general framework for mixed tiling systems to match the tiling iterated function setting described in previous chapters. The presentation and packaging of these ideas is original. Section 5.2 discusses one-dimensional mixed systems under this symbolic lens and builds up to stating the main cohomology result of [GM13]. Then section 5.3 looks at the fractal pinwheel tiling as a two-dimensional mixed example and relates the neighbour map theory. Section 5.4 presents a mixed Sierpinksi gasket example that shows how the theory also caters for fractal tiles with no interior. In section 5.5 we explore how these ideas are related to the V-variable and superfractal theory discussed in [Bar06] and [FHH15].

This chapter ties together the work from all the previous chapters. We link back to the A & P theory with reference to cohomology calculations of tiling spaces and the work of Bandt with the inclusion of neighbour graphs. Additionally, we keep the symbolic perspective strong and show that the theory holds for truely fractal tilings. Scattered throughout this chapter we pinpoint some potential avenues for further research.

5.1 Notation and Set-up

Let $\hat{\mathcal{F}} = \{\mathcal{F}_{(1)}, ...\mathcal{F}_{(N)}\}$ for $N \geq 2$ be a family of tiling IFSs where the combined set of contractive similitudes have scaling factors which are integer powers of some $0 < s < 1$. For our purposes we place additional constraints on this family, though we suspect a more general framework could work. We assume that all the graphs $\mathcal{G}_{(i)}$ for $i \in \{1, ...N\}$ have the same number of vertices and that the attractor components are compatible in some nice way. We have not been able to neatly capture the attractor compatibility requirement so we will handle it for now on a case-by-case basis. A more formal description of this set-up is defined for the case when $N = 2$, which covers all the examples presented in this thesis.

Definition 5.1. Let $\hat{\mathcal{F}} = \{\mathcal{F}, \tilde{\mathcal{F}}\}$ be a family of two tiling graph IFSs such that all maps $f_i \in \mathcal{F}$ with $i \in \{1, ...|\mathcal{F}|\}$ and $f_{\tilde{j}} \in \mathcal{F}$ with $j \in \{1, ...|\tilde{\mathcal{F}}|\}$ have scaling factors that are integer powers of some $0 < s < 1$. For graphs $\mathcal{G}$ and $\tilde{\mathcal{G}}$ we require that $|\mathcal{V}| = |\tilde{\mathcal{V}}| = p$ and the vertices are matched with respect to the compatible attractor components (as stated above, we expand on this when clarification is necessary). Let $\hat{\mathcal{G}}$ denote the graph with its edge set the union of edges from $\mathcal{G}$ and $\tilde{\mathcal{G}}$. We like to think of directed paths in $\hat{\mathcal{G}}$ as paths that can jump between $\mathcal{G}$ and $\tilde{\mathcal{G}}$ on the identified vertices. If these conditions hold, then we call $(\hat{\mathcal{F}}, \hat{\mathcal{G}})$ a mixed tiling IFS.

Let $\hat{\Sigma}_k$ be the set of directed paths in $\hat{\mathcal{G}}$ of length $k \in \mathbb{N}$ and $\hat{\Sigma}_\infty$ be the set of directed paths of infinite length. We define $\hat{\Sigma}_* := \cup_{k\in\mathbb{N}} \hat{\Sigma}_k$ and $\hat{\Sigma} := \hat{\Sigma}_* \cup \hat{\Sigma}_\infty$. Also, $\hat{\Sigma}^v_* = \{\sigma \in \hat{\Sigma}_* : \overleftarrow{v}(\sigma_1) = v\}$ is the set of finite paths that start at a specified vertex . As before, we let $\hat{\mathcal{G}}^\dagger$ be the graph whose edges go in the opposite direction to $\hat{\mathcal{G}}$. We define $\hat{\Sigma}^\dagger_k$, $\hat{\Sigma}^\dagger_\infty$, $\hat{\Sigma}^\dagger_*$ and $\hat{\Sigma}^\dagger$ in the obvious way.

Example 5.2. To help concretely explain our new definitions, we keep in mind an example mixed IFS of the form $\hat{\mathcal{F}} = \{\mathcal{F}, \tilde{\mathcal{F}}\}$ with $\mathcal{F} = \{f_1, f_2\}$ and $\tilde{\mathcal{F}} = \{f_{\tilde{1}}, f_{\tilde{2}}\}$. Maps $f_1, f_{\tilde{1}}$ have scaling factor s and maps $f_2, f_{\tilde{2}}$ have scaling factor s^2 for some $0 < s < 1$. So edges in $\mathcal{G}$ are labelled from the set $\{1, 2\}$ and edges in $\tilde{\mathcal{G}}$ are labelled from the set $\{\tilde{1}, \tilde{2}\}$.

Definition 5.3. Let $\theta \in \hat{\Sigma}_k$. For $1 \leq i \leq k$, define $\mathcal{G}_{\theta_i} = \mathcal{G}$ if $f_{\theta_i} \in \mathcal{F}$ or $\mathcal{G}_{\theta_i} = \tilde{\mathcal{G}}$ if $f_{\theta_i} \in \tilde{\mathcal{F}}$.

Definition 5.4. Let $\sigma \in \hat{\Sigma}_k$. We define an ordered sequence $t^\sigma = \{t_i^\sigma\}_{i=1}^n$ with $t_1^\sigma = 0$, $\{t_i^\sigma\}_{i=2}^{n-1}$ corresponding to the sequence of natural numbers $\{m\}$ such that $\mathcal{G}_{\sigma_m} \neq \mathcal{G}_{\sigma_{m+1}}$ for $m \in \{1, ...k-1\}$ and $t_n^\sigma = |\sigma|$. We call t^σ the jump sequence of σ. Let $|t^\sigma|$ denote the length of the sequence.

Example 5.5. For the IFS set up in Example 5.2, consider the path $\theta = 11\tilde{2}111\tilde{1}\tilde{1}$. As always $t_1^\theta = 0$. Since $\mathcal{G}_2 \neq \mathcal{G}_3$, $\mathcal{G}_3 \neq \mathcal{G}_4$, $\mathcal{G}_6 \neq \mathcal{G}_7$, $\{t_2^\theta, t_3^\theta, t_4^\theta\} = \{2, 3, 6\}$ and $t_5^\theta = 8$. So θ has jump sequence $t^\theta = \{0, 2, 3, 6, 8\}$. Another path $\psi = 2\tilde{1}\tilde{1}12\tilde{2}$ has jump sequence $t^\psi = \{0, 1, 3, 5, 6\}$.

Definition 5.6. We define an equivalence relation on strings $\sigma, \omega \in \hat{\Sigma}_*$ by $\sigma \sim \omega$ if $\sigma, \omega \in \hat{\Sigma}_*^v$ and $\xi(\sigma_{t_i^\sigma+1}...\sigma_{t_{i+1}^\sigma}) = \xi(\omega_{t_i^\omega+1}...\omega_{t_{i+1}^\omega})$ for all $i \in \{1, ...n\}$ with $n = |t^\sigma| - 1 = |t^\omega| - 1$. We denote the equivalence class by $[\sigma]$.

The equivalence relation identifies two finite strings if they start in the same graph and the total scaling between all the jumps from one graph to the other are equal.

Example 5.7. Consider the two strings $\theta = 11\tilde{2}111\tilde{1}\tilde{1}$ and $\psi = 2\tilde{1}\tilde{1}12\tilde{2}$ from before. We observe that $\xi(\theta_1\theta_2) = \xi(\psi_1) = 2$, $\xi(\theta_3) = \xi(\psi_2\psi_3) = 2$, $\xi(\theta_4\theta_5\theta_6) = \xi(\psi_4\psi_5) = 3$ and $\xi(\theta_7\theta_8) = \xi(\psi_6) = 2$. Thus, $\theta \sim \psi$ since the strings start in the same graph and have equal scaling totals between graph jumps.

Definition 5.8. For $\sigma \in \hat{\Sigma}_*$ define $\Omega_{[\sigma]} := \{\omega \in \hat{\Sigma}_*^{\overleftarrow{v}(\sigma_1)} : \xi^-(\omega) \leq \xi(\sigma) < \xi(\omega)$ and $\xi^-(\omega|_{t_i^\omega}) \leq \xi(\sigma|_{t_i^\sigma}) < \xi(\omega|_{t_i^\omega}), i \in \{2, ...|t^\omega| - 1\}\}$.

Definition 5.8 is a generalisation of Definition 1.15 from chapter 1. The additional requirement in the mixed setting is that we must also keep track of the scaling between graph jumps.

Example 5.9. Let us compute $\Omega_{[\tilde{2}1]}$ for our working example. We know that all strings must start at the sole vertex in $\tilde{\mathcal{G}}$ and satisfy $\xi^-(\omega|_{t_2^\omega}) \leq \xi(\tilde{2}) < \xi(\omega|_{t_2^\omega})$. Since $\xi(\tilde{2}) = 2$, the possible initial sub-strings are $\tilde{2}\tilde{2}, \tilde{1}\tilde{1}\tilde{2}, \tilde{2}\tilde{1}, \tilde{1}\tilde{2}, \tilde{1}\tilde{1}\tilde{1}$. Since $\xi(\tilde{2}\tilde{2}) = \xi(\tilde{1}\tilde{1}\tilde{2}) > \xi(\tilde{2}1)$, the strings $\tilde{2}\tilde{2}$ and $\tilde{1}\tilde{1}\tilde{2}$ are already in our set without jumping to the other graph. For the rest of the set, we find the strings that jump to $\mathcal{G}$ and satisfy $\xi^-(\omega) \leq \xi(\tilde{2}1) < \xi(\omega)$. It works out that

$$\Omega_{[\tilde{2}1]} = \{\tilde{2}\tilde{2}, \tilde{1}\tilde{1}\tilde{2}, \tilde{2}\tilde{1}1, \tilde{2}\tilde{1}2, \tilde{1}\tilde{2}1, \tilde{1}\tilde{2}2, \tilde{1}\tilde{1}\tilde{1}1, \tilde{1}\tilde{1}\tilde{1}2\}$$

is the complete set.

The next basic lemma follows directly from the definitions.

Lemma 5.10. *If $\omega \in [\sigma]$ then $\Omega_{[\sigma]} = \Omega_{[\omega]}$.*

Proof. Suppose $\omega \sim \sigma$. Then $\overleftarrow{v}(\sigma_1) = \overleftarrow{v}(\omega_1)$ and for some $m \in \mathbb{N}$, $|t^\sigma| = |t^\omega| = m$, and $\xi(\sigma|_{t_i^\sigma}) = \xi(\omega|_{t_i^\omega})$ for all $i \in \{1, ...m\}$. Then by definition,

$$\begin{aligned}\Omega_{[\sigma]} &= \{\theta \in \hat{\Sigma}_*^{\overleftarrow{v}(\sigma_1)} : \xi^-(\theta) \leq \xi(\sigma) < \xi(\theta),\, \xi^-(\theta|_{t_i^\theta}) \leq \xi(\sigma|_{t_i^\sigma}) < \xi(\theta|_{t_i^\theta}), i \in \{2, ...|t^\theta| - 1\}\} \\ &= \{\theta \in \hat{\Sigma}_*^{\overleftarrow{v}(\omega_1)} : \xi^-(\theta) \leq \xi(\omega) < \xi(\theta),\, \xi^-(\theta|_{t_i^\theta}) \leq \xi(\omega|_{t_i^\omega}) < \xi(\theta|_{t_i^\theta}), i \in \{2, ...|t^\theta| - 1\}\} \\ &= \Omega_{[\omega]}\end{aligned}$$

□

Ultimately, we want elements in the set $\Omega_{[\sigma]}$ to correspond to the set of relative addresses in a bounded tiling. That is, these sets provide a symbolic partition of the tiling. Then to fill in the points inside every tile we need to define a unique compact set whose support blown up is the support of the bounded tiling and a coding map that gives an appropriate address space structure to this subset. For the address space, we define sets of strings that are either prefixes of some element in $\Omega_{[\sigma]}$ or the strings have a prefix that lies in some $\Omega_{[\sigma]}$ and the remaining string stays in the same graph where the prefix ends.

Definition 5.11. For $\sigma \in \hat{\Sigma}_*$ and $k \in \mathbb{N}$ define

$$\begin{aligned}\Omega_{[\sigma]}^k &:= \{\omega \in \hat{\Sigma}_* : |\omega| = k \text{ and } (\exists \gamma \in \Omega_{[\sigma]} \text{ s.t. } \omega \sqsubseteq \gamma \text{ or} \\ &\quad \exists l \leq k \in \mathbb{N} \text{ s.t. } \omega|l \in \Omega_{[\sigma]}, S^l\omega \in G_{\omega_l})\}, \\ \Omega_{[\sigma]}^* &:= \cup_{k\in\mathbb{N}} \Omega_{[\sigma]}^k, \\ \Omega_{[\sigma]}^\infty &:= \{\omega \in \hat{\Sigma}_\infty : \exists l \in \mathbb{N}\ \omega|l \in \Omega_{[\sigma]}, S^l\omega \in G_{\omega_l}\}, \text{ and} \\ \hat{\Omega}_{[\sigma]} &:= \Omega_{[\sigma]}^* \cup \Omega_{[\sigma]}^\infty.\end{aligned}$$

Definition 5.12. For $\sigma \in \hat{\Sigma}_*$ define $A_{[\sigma]} \in \mathbb{H}(\mathbb{X})$ as the compact subset such that

$$A_{[\sigma]} := \bigcup_{\omega \in \Omega_{[\sigma]}} f_\omega(A_{\overrightarrow{v}(\omega_{|\omega|})}).$$

It follows from Lemma 5.10 that if $\omega \in [\sigma]$ then $A_{[\sigma]} = A_{[\omega]}$. We have defined the set $A_{[\sigma]}$ so that $\Omega_{[\sigma]}$ gives a symbolic partition of the set. The set $\hat{\Omega}_{[\sigma]}$ is defined so that it gives a full address space structure on the set of compact subsets of $A_{[\sigma]}$.

Definition 5.13. For $\sigma \in \hat{\Sigma}_*$ define the map $\hat{\pi}_{[\sigma]} : \hat{\Omega}_{[\sigma]} \to \mathbb{H}(A_{[\sigma]})$ as

$$\begin{aligned}\hat{\pi}_{[\sigma]}(\omega) &= f_\omega(A_{\overrightarrow{v}(\omega_{|\omega|})}) \text{ for all } \omega \in \Omega_{[\sigma]}^k \text{ with } k \in \mathbb{N} \\ \hat{\pi}_{[\sigma]}(\gamma) &= \lim_{k\to\infty} \hat{\pi}_{[\sigma]}(\gamma|k) \text{ for all } \gamma \in \Omega_{[\sigma]}^\infty.\end{aligned}$$

Restricted to strings of infinite length, $\hat{\pi}_{[\sigma]}(\Omega_{[\sigma]}^\infty) = A_{[\sigma]}$.

The idea for the mixed tiling map is that for any $\theta \in \hat{\Sigma}^{\dagger}_{*}$ the set $\Omega_{[\theta^{\dagger}]}$ corresponds to the set of relative addresses of the tiles. The map $\hat{\pi}_{[\theta^{\dagger}]}$ realises the codes in $\Omega_{[\theta^{\dagger}]}$ as subsets of the attractor $A_{[\theta^{\dagger}]}$. Applying the expansive function $f_{-\theta}$ blows the tiles back up to appropriate sizes.

Definition 5.14. The mixed tiling map $\hat{\Pi} : \hat{\Sigma}^{\dagger} \to \mathbb{H}(\mathbb{H}(\mathbb{R}^m))$ is defined by

$$\hat{\Pi}(\theta_1\theta_2...\theta_k) := \{f_{-\theta_1...\theta_k}\hat{\pi}_{[\theta^{\dagger}]}(\sigma) : \sigma \in \Omega_{[\theta^{\dagger}]}\}$$

for $\theta = \theta_1...\theta_k \in \hat{\Sigma}^{\dagger}_{*}$ and

$$\hat{\Pi}(\theta) := \lim_{k\to\infty} \hat{\Pi}(\theta_1\theta_2...\theta_k)$$

for $\theta \in \hat{\Sigma}^{\dagger}_{\infty}$.

Remark 5.15. We explain how these definitions match the tiling IFS setting presented in chapter 1 if we consider a string that stays in one graph. Let $\theta \in \Sigma^{\dagger}_{*} \subset \hat{\Sigma}^{\dagger}_{*}$ such that $|\theta| = k$. So θ is a string of length k in the graph $\mathcal{G}^{\dagger}$ that never jumps to the other graph. Then

$$\begin{aligned}\Omega_{[\theta^{\dagger}]} &= \{\omega \in \hat{\Sigma}^{v}_{*} : \xi^{-}(\omega) \le \xi(\theta^{\dagger}) < \xi(\omega) \text{ and } \mathcal{G}_{\omega_i} = \mathcal{G}\ \forall 1 \le i \le |\omega|\}\\ &= \{\omega \in \Sigma^{v}_{*} : \xi^{-}(\omega) \le \xi(\theta^{\dagger}) < \xi(\omega)\}\\ &= \{\omega \in \Sigma^{v}_{*} : \xi^{-}(\omega) \le \xi(\theta) < \xi(\omega)\}\\ &= \Omega^{v}_{\theta},\end{aligned}$$

where $v = \overleftarrow{v}(\theta^{\dagger}_1) = \overrightarrow{v}(\theta_k)$ is the unique vertex such that θ_k is a directed edge in $\mathcal{G}^{\dagger}$ to v. Also

$$\begin{aligned}\hat{\Omega}_{[\theta^{\dagger}]} &= \hat{\Omega}^{*}_{[\theta^{\dagger}]} \cup \hat{\Omega}^{\infty}_{\theta^{\dagger}]}\\ &= \Sigma_{*} \cup \Sigma_{\infty}\\ &= \Sigma,\\ A_{[\theta^{\dagger}]} &= A,\\ \hat{\pi}_{[\theta^{\dagger}]} &= \pi\end{aligned}$$

where A is the attractor of the IFS $(\mathcal{F}, \mathcal{G})$ and $\pi : \Sigma \to \mathbb{H}(A)$ is the usual coding map for A. Hence,

$$\begin{aligned}\hat{\Pi}(\theta) &= \{f_{-\theta}\hat{\pi}_{[\theta^{\dagger}]}(\sigma) : \sigma \in \Omega_{[\theta^{\dagger}]}\}\\ &= \{f_{-\theta}\pi(\sigma) : \sigma \in \Omega^{v}_{\xi(\theta)}\}\\ &= \Pi(\theta)\end{aligned}$$

where $\Pi : \Sigma^{\dagger} \to \mathbb{H}(\mathbb{H}(\mathbb{R}^M))$ is the original tiling map from Definition 1.16.

For convenience, let $\hat{\mathbb{T}}_* := \hat{\Pi}(\hat{\Sigma}^\dagger_*)$ and $\hat{\mathbb{T}}_\infty := \hat{\Pi}(\hat{\Sigma}^\dagger_\infty)$ be the set of tilings made from strings of finite and infinite length respectively. Let $\hat{\mathbb{T}} := \hat{\Pi}(\hat{\Sigma}^\dagger)$ be the union of these sets.

Definition 5.16. We also define canonical mixed tilings for $\sigma \in \hat{\Sigma}_*$ by

$$T_{[\sigma]} := s^{-\xi(\sigma)} \hat{\pi}_{[\sigma]}(\Omega_{[\sigma]})$$

with

$$\operatorname{supp}(T_{[\sigma]}) = s^{-\xi(\sigma)} A_{[\sigma]}.$$

The statement and proof of the following theorem closely resembles Theorem 1.24.

Theorem 5.17. *For all* $\theta \in \hat{\Sigma}^\dagger_*$,

$$\hat{\Pi}(\theta) = E_\theta T_{[\theta^\dagger]}$$

for $E_\theta = f_{-\theta} s^{\xi(\theta)}$.

Proof. Suppose $|\theta| = k$. Then

$$\begin{aligned}
\hat{\Pi}(\theta) &= f_{-\theta_1 \dots \theta_k} \{\hat{\pi}_{[\theta^\dagger]}(\sigma) : \sigma \in \Omega_{[\theta^\dagger]}\} \\
&= f_{-\theta_1 \dots \theta_k} s^{\xi(\theta)} s^{-\xi(\theta)} \{\hat{\pi}_{[\theta^\dagger]}(\sigma) : \sigma \in \Omega_{[\theta^\dagger]}\} \\
&= E_\theta s^{-\xi(\theta^\dagger)} \hat{\pi}_{[\theta^\dagger]}(\Omega_{[\theta^\dagger]}) \\
&= E_\theta T_{[\theta^\dagger]}.
\end{aligned}$$

□

Remark 5.18. We discuss some properties of tilings in the set $\hat{\mathbb{T}}$. Just as in the original setting, each set $\hat{\Pi}(\theta)$ in $\hat{\mathbb{T}}$ is a tiling of a subset of $\mathbb{R}^M$, the subset being bounded when $\theta \in \hat{\Sigma}^\dagger_*$ and unbounded when $\theta \in \hat{\Sigma}^\dagger_\infty$. However, it is not necessarily the case that the sequence of tilings $\{\Pi(\theta|k)\}_{k=1}^\infty$ is nested for an arbitrary $\theta \in \hat{\Sigma}^\dagger_\infty$. We show some counter-examples to the nesting property in the next section. Let A_v and $\tilde{A}_v$ for $v \in \mathcal{V}$ denote the attractor components of $(\mathcal{F}, \mathcal{G})$ and $(\tilde{F}, \tilde{G})$ respectively. Let $a_{\max}$ and $\tilde{a}_{\max}$ denote the maximum scaling factors in the respective IFS. The tiling map is constructed in such a way that the prototile set for any tiling in $\hat{\mathbb{T}}$ is contained within the set

$$\mathcal{P} = \{s^i A_v, s^i \tilde{A}_v : i \in \{1, 2, \max(a_{\max}, \tilde{a}_{\max})\}$$

though we suspect a more precise description of this prototile set is possible.

5.2 One-Dimensional Mixed Tilings

One-dimensional tilings have been studied thoroughly (see [BD08] and [Rus16] for example) and in recent years there has been a growing interest in the relevant mixed tiling systems. We check that the theory defined in the previous section constructs appropriate one-dimensional tilings. At the end of this section, we state the main cohomology result in [GM13] which provides a convincing reason why these mixed systems are interesting.

5.2.1 Mixed Fibonacci

In section 1.4.1 we defined the Fibonacci IFS by $\mathcal{F} = \{f_1, f_2\}$ with attractor the unit interval I and prototile set $\{a, b\}$. Figure 1.4 displays tilings $\Pi(1)$ and $\Pi(2)$ with their relative addresses labelled.

Another one-dimensional IFS that produces Fibonacci tilings is $\tilde{\mathcal{F}} = \{f_{\tilde{1}}, f_{\tilde{2}}\}$ with maps defined as

$$f_{\tilde{1}}(x) = sx + s^2 \text{ and } f_{\tilde{2}}(x) = s^2 x.$$

The support of the attractor is again I and we observe that $f_{\tilde{1}}(I) = a$ and $f_{\tilde{2}}(I) = b$ so this tiling has the same prototile set as $\mathcal{F}$. Figure 5.1 displays the tilings $\Pi(\tilde{1})$ and $\Pi(\tilde{2})$ with the relative addresses labelled.

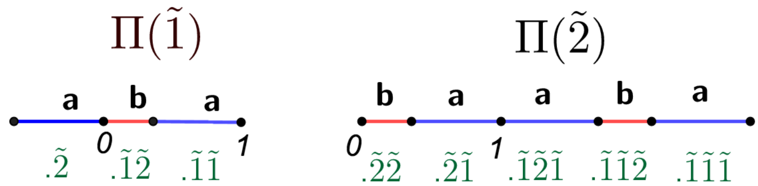

Figure 5.1: Fibonacci tilings $\Pi(\tilde{1})$ and $\Pi(\tilde{2})$

In this example, the support of both attractor components is the unit interval so for whatever compatibility notion we require these must be compatible. Together $\hat{\mathcal{F}} = \{\mathcal{F}, \tilde{\mathcal{F}}\}$ satisfies the conditions in Definition 5.1 for a mixed tiling IFS. We call the tilings from $\hat{\mathcal{F}}$ mixed Fibonacci tilings. The example strung through the previous section was made, with convenient foresight, to match the structure of this mixed tiling IFS.

Applying Definition 5.14 for the mixed tiling map, we compute example bounded tilings $\hat{\Pi}(1\tilde{2})$ and $\hat{\Pi}(1\tilde{1}\tilde{1})$. By definition

$$\hat{\Pi}(1\tilde{2}) = \{f_{-1\tilde{2}}\hat{\pi}_{[\tilde{2}1]}(\sigma) : \sigma \in \Omega_{[\tilde{2}1]}\}.$$

In Example 5.9 we computed $\Omega_{[\tilde{2}1]} = \{\tilde{2}\tilde{2}, \tilde{1}\tilde{1}\tilde{2}, \tilde{2}\tilde{1}1, \tilde{2}\tilde{1}2, \tilde{1}\tilde{2}1, \tilde{1}\tilde{2}2, \tilde{1}\tilde{1}\tilde{1}1, \tilde{1}\tilde{1}\tilde{1}2\}$. So the tiling $\hat{\Pi}(1\tilde{2})$ (displayed in Figure 5.2) is made from eight tiles with the elements of $\Omega_{[\tilde{2}1]}$ corresponding bijectively to the set of relative addresses. It is clear that $\hat{\Pi}(1)$ is not nested in this bounded tiling.

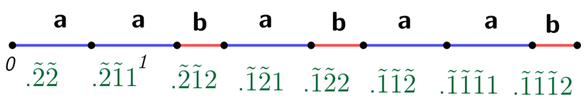

Figure 5.2: Mixed Fibonacci tiling $\hat{\Pi}(1\tilde{2})$

Similarly, we consider

$$\hat{\Pi}(1\tilde{1}\tilde{1}) = \{f_{-1\tilde{1}\tilde{1}}\hat{\pi}_{[\tilde{1}\tilde{1}1]}(\sigma) : \sigma \in \Omega_{[\tilde{1}\tilde{1}1]}\}.$$

Since $\tilde{1}\tilde{1}1 \sim \tilde{2}1$, we know that $\Omega_{[\tilde{1}\tilde{1}1]} = \Omega_{[\tilde{2}1]}$. So $\hat{\Pi}(\tilde{1}\tilde{1}1)$ (displayed in Figure 5.3) is made from the same tiles as $\Omega_{[\tilde{2}1]}$ with identical relative addresses but translated to the left.

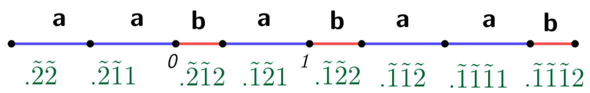

Figure 5.3: Mixed Fibonacci tiling $\hat{\Pi}(1\tilde{1}\tilde{1})$

Both of these tiles are isometries of the canonical tiling

$$T_{[\tilde{2}1]} = s^{-\xi(\sigma)}\hat{\pi}_{[\tilde{2}1]}(\Omega_{[\tilde{2}1]}).$$

5.2.2 Mixed Decorated Halves

In their paper, G & M define

$$\phi_1 : \begin{array}{ccc} a & \to & ab \\ b & \to & bc \\ c & \to & ca \end{array} \quad \text{and} \quad \phi_2 : \begin{array}{ccc} a & \to & bb \\ b & \to & cc \\ c & \to & ac \end{array}$$

as two substitution maps in a mixed substitution tiling system [GM13]. We translate this system into our setting by defining two graph IFSs: $\mathcal{F}$ for ϕ_1 and $\tilde{\mathcal{F}}$ for ϕ_2. All the maps are have scaling factor $\frac{1}{2}$ and either no translation or translation by $\frac{1}{2}$.

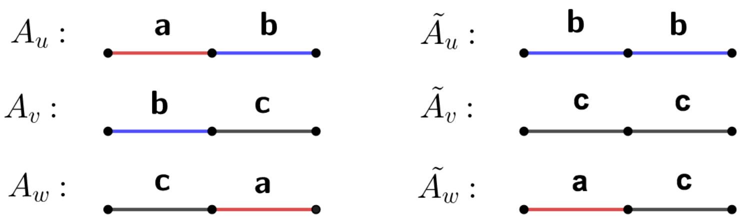

Figure 5.4: Mixed decorated halves attractor components

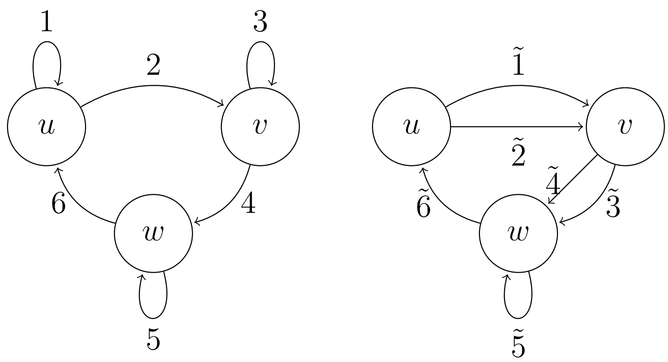

Figure 5.5: Mixed decorated halves graphs $\mathcal{G}$ and $\tilde{\mathcal{G}}$

The graphs $\mathcal{G}$ and $\tilde{\mathcal{G}}$, displayed in Figure 5.5, provide the labelling of the maps for the attractor components (see Figure 5.4). Both $\mathcal{F}$ and $\tilde{\mathcal{F}}$ have prototile sets $\{a, b, c\}$. We name this mixed tiling IFS the mixed decorated halves. This example does not have any interesting geometry. We think of the real line as being decorated with the labelled intervals $\{a, b, c\}$, each with length $\frac{1}{2}$.

As noted in chapter 1, for each graph IFS, it is possible to translate the attractor components to be disjoint on one copy of $\mathbb{R}$ by a change of coordinates. For simplicity we keep the three copies of $\mathbb{R}$ so that the support of each attractor component is the unit interval I. We do not lose anything in this discussion by this adaptation.

Applying Definition 5.14 we construct the bounded tiling $\hat{\Pi}(5\tilde{5})$ displayed in Figure 5.6. Following the computations we have seen numerous times now, we find the set

$$\Omega_{[\tilde{5}5]} = \{\tilde{6}\tilde{1}3, \tilde{6}\tilde{1}4, \tilde{6}\tilde{2}3, \tilde{6}\tilde{2}4, \tilde{5}\tilde{6}1, \tilde{5}\tilde{6}2, \tilde{5}\tilde{5}5, \tilde{5}\tilde{5}6\}$$

which is in bijective correspondence with the set of relative addresses.

We know $\tilde{5}5 \sim \tilde{5}6 \sim \tilde{6}1 \sim \tilde{6}2$ since all the strings start at vertex $w \in \tilde{\mathcal{G}}$ and have the same scaling length between graph jumps. It follows that $\Omega_{[\tilde{5}5]} = \Omega_{[\tilde{5}6]} =$

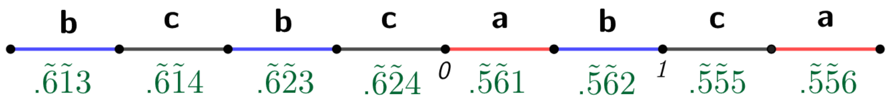

Figure 5.6: Mixed decorated halves tiling $\hat{\Pi}(5\tilde{5})$

$\Omega_{[\tilde{6}1]} = \Omega_{[\tilde{6}2]}$ and so $\hat{\Pi}(6\tilde{5})$, $\hat{\Pi}(1\tilde{6})$ and $\hat{\Pi}(2\tilde{6})$ are all translations of $\hat{\Pi}(5\tilde{5})$.

Now we shift our focus to presenting the cohomology result in [GM13] for this mixed tiling system. The substitution tiling spaces Δ considered by G & M satisfies the same conditions as required by A & P: ω is invertible, the substitution is primitive, and the tilings satisfy a finite pattern condition. To generalise the notion of a substitution tiling space by allowing more than one substitution to be used, G & M define mixed substitution spaces.

Definition 5.19. Let $\mathcal{S} = \{\phi_1, \phi_2 \cdots \phi_N\}$ be a finite set of substitutions all acting on the same prototile set $\mathcal{P} = \{p_1, p_2 \cdots p_l\}$ in $\mathbb{R}^M$ and consider an infinite sequence $s = (s_1, s_2, \cdots) \in [N]^\infty$. Let $\hat{\Delta}$ denote the set of all tilings containing only translations of the prototiles. Then the mixed subsitution space of $\mathcal{S}$ and s denoted by Δ_s consists of all tilings $T \in \hat{\Delta}$ such that every patch $P \subseteq T$ is contained in $\phi_{s_1}\phi_{s_2}\cdots\phi_{s_n}(p_i+u)$ for some $n \in \mathbb{N}$, prototile p_i, and vector $u \in \mathbb{R}^M$.

In [GM13], the authors construct a universal inverse limit system (in the style of A & P) which allows them to compute the Čech cohomology of these mixed tiling spaces. For the mixed decorated halves example, considered as the substitution system $\{\phi_1, \phi_2\}$ defined at the beginning of this subsection, they show that the rank of the first cohomology group of the spaces Δ_s depends on the string $s \in [2]^\infty$. Specifically they compute

$$\text{rank } H^1(\Delta_s) = \begin{cases} 7 & \text{if } s \text{ contains only finitely many 2s} \\ 5 & \text{if } s \text{ contains only finitely many strings of the form } 21^{3i}2 \\ 3 & \text{if } s \text{ contains infinitely many strings of the form } 21^{3i}2. \end{cases}$$

For some $s_1, s_2 \in [2]^\infty$ the spaces Δ_{s_1} and Δ_{s_2} can be distinguished by the rank of their cohomology groups. Ideally we would like to interpret this result in the language of the mixed tiling IFS framework. So to end this section we propose a definition and make a remark concerning the translation between these two settings. These ideas are still conjectural and need to be carefully checked.

Definition 5.20. Let $\hat{\mathcal{F}}$ be called a mixed substitution IFS if $\hat{\mathcal{F}}$ is a mixed tiling IFS by Definition 5.1 and both $(\mathcal{F}, \mathcal{G})$ and $(\tilde{\mathcal{F}}, \tilde{\mathcal{G}})$ are substitution IFSs by Definition 5.20. For $\theta \in \hat{\Sigma}^{\dagger}_{\infty}$, define $\Delta_{[\theta]} = \{\hat{\Pi}(\sigma) + n : \sigma \in [\theta], n \in \mathbb{R}^M\}$ as the mixed substitution tiling space.

Remark 5.21. By defining spaces of this form, it should be possible to neatly translate the cohomology result of G & M in terms of the equivalence class of θ. That is, the rank of the first cohomology group depends on how θ scales and jumps between the graphs.

5.3 Fractal Pinwheel Tilings

Bandt, Mekhontsev, and Tetenov's recent paper [BMT18] presents an unexpected single fractal tile with irrational rotations, which they call the fractal pinwheel tiling.

Definition 5.22. A compact set $A \subset \mathbb{R}^M$ is called a reptile if there exists a similarity map g and isometries $\{h_1, ...h_N\}$ such that

$$g(A) = h_1(A) \cup ... \cup h_N(A),$$

and any pair of sets $h_i(A)$ share no interior points.

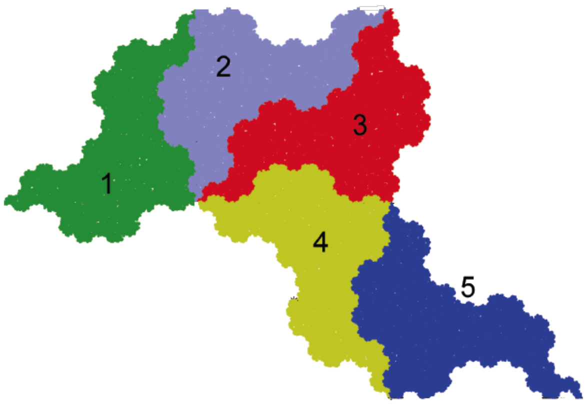

Figure 5.7: Fractal Pinwheel Attractor [BMT18]

For the first fractal pinwheel tiling, pictured in Figure 5.7, the maps are

$$g\begin{pmatrix}x\\y\end{pmatrix}=\begin{pmatrix}2x+y\\x-2y\end{pmatrix},$$

$$h_1\begin{pmatrix}x\\y\end{pmatrix}=\begin{pmatrix}x\\y\end{pmatrix},h_2\begin{pmatrix}x\\y\end{pmatrix}=\begin{pmatrix}y+1\\x\end{pmatrix},h_3\begin{pmatrix}x\\y\end{pmatrix}=\begin{pmatrix}2-y\\1-x\end{pmatrix},h_4\begin{pmatrix}x\\y\end{pmatrix}=\begin{pmatrix}x+1\\-y\end{pmatrix},h_5\begin{pmatrix}x\\y\end{pmatrix}=\begin{pmatrix}y+2\\-x\end{pmatrix}.$$

Then the set $f_i = g^{-1}h_i$ for $i = 1, \ldots 5$

$$\frac{1}{5}\begin{pmatrix}2x+y\\x-2y\end{pmatrix},\frac{1}{5}\begin{pmatrix}x+2y+2\\-2x+y+1\end{pmatrix},\frac{1}{5}\begin{pmatrix}-x-2y+5\\2x-y\end{pmatrix},\frac{1}{5}\begin{pmatrix}2x-y+2\\x+2y+1\end{pmatrix},\frac{1}{5}\begin{pmatrix}-x+2y+4\\2x+y+2\end{pmatrix}$$

defines an IFS $\mathcal{F}$ whose contractive maps all have scaling factor $\frac{1}{5}$. Applying the neighbour graph technique (see chapter 4) we summarise the findings and discussion from [BMT18] and describe properties of this fractal pinwheel tiling. This tiling has two kinds of neighbours: point neighbours, which meet on a single point, and edge neighbours, which meet on uncountably many points. Using the IFStile computer software [Mek] the authors find 11 edge neighbours and 69 point neighbours. We restrict our attention to the neighbour graph of the edge neighbours.

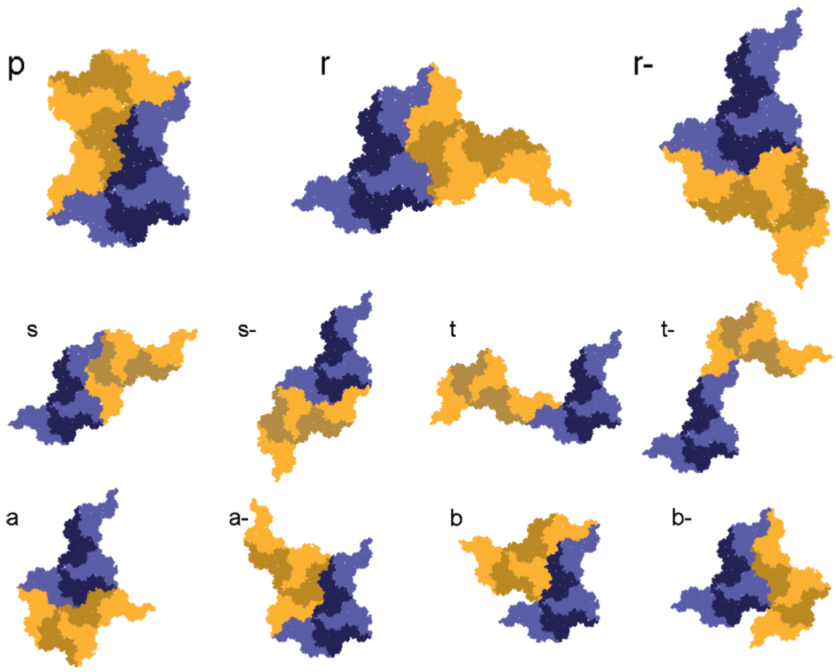

Figure 5.8: Fractal Pinwheel Edge Neighbours [BMT18]

From the identity vertex, three rational rotation neighbour maps can be reached: $p = h_2^{-1}h_3$, $r = h_3^{-1}h_4$ and $r^- = h_4^{-1}h_3$. The neighbour p is a 180° rotation and hence self-inverse. The neighbour r is a clockwise 90° rotation and its inverse r^{-} is a counterclockwise 90° rotation. Studying the neighbouring subpieces, the directed edges for the sub-neighbour graph (see Figure 5.9) with these three vertices are found.

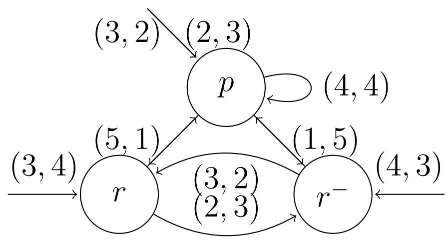

Figure 5.9: Fractal pinwheel sub-neighbour graph

From the identity, there are edges in the neighbour graph to the vertex corresponding to the glide reflection $s = h_4^{-1}h_5$ and its inverse. There is another glide reflection from the subpieces A_{15} and A_{21} given by $t = f_{15}^{-1}f_{21}$ and its inverse. Subpieces A_{13} and A_{21} yield an irrational rotation map $a = f_{13}^{-1}f_{21}$ and subpieces A_{15} and A_{22} yield another irrational rotation $b = f_{15}^{-1}f_{22}$. The complete set of 11 edge neighbours is

$$\mathcal{N} = \{p, r, r^{-1}, s, s^{-1}, t, t^{-1}, a, a^{-1}, b, b^{-1}\}$$

all displayed in Figure 5.8.

The authors were most excited by the existence of irrational rotation neighbour maps. Irrational rotations imply statistical circular symmetry of rotations [Fre08]. The pinwheel triangle tiling was the first example where it was proved that the orientations of triangles in an infinite tiling are equidistributed on the circle [Rad99]. In the tiling IFS language, this means that for any unbounded tiling in the image of Π the orientation of the tiles are dense in $[0, 2\pi]$. The fractal pinwheel tiling is interesting because it shares this statistical circular symmetry property with the original pinwheel tiling but the attractor is bounded by a closed Jordan curve of dimension $\frac{\log(1+\sqrt{2})}{\log(\sqrt{5})}$ [BMT18]. However, recalling back to chapter 3, we cannot take this IFS and form a substitution IFS to match the A & P setting. There is no way to construct a finite prototile set so that all tiles are mapped from the prototile set to any fractal pinwheel tiling by translation.

In [BMT18] a second fractal pinwheel tiling is presented. The authors observe that the union of pieces A_2 and A_3 is mapped to itself by the reflection

$$\sigma \begin{pmatrix} x \\ y \end{pmatrix} = \begin{pmatrix} x \\ 1-y \end{pmatrix}.$$

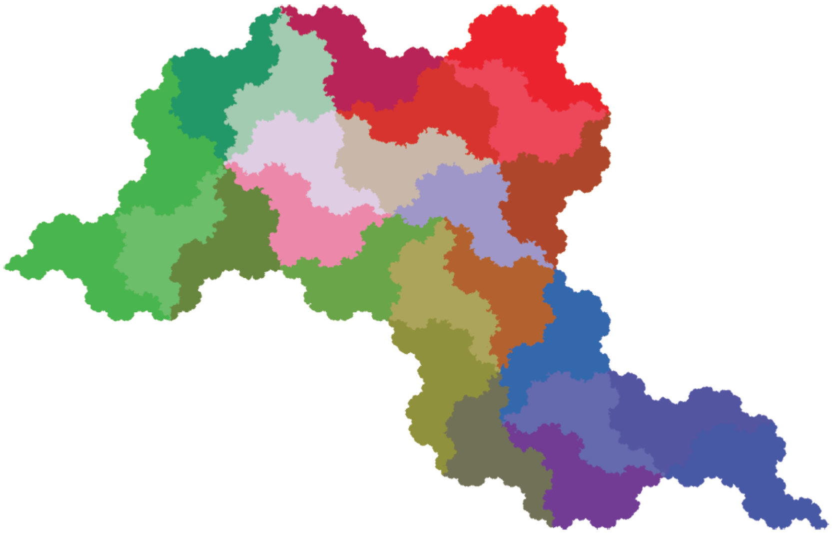

Figure 5.10: Second subdivison of second fractal pinwheel [BMT18]

New isometries are defined as

$$h_{\tilde{2}} = \sigma h_2 = \begin{pmatrix} y+1 \\ 1-x \end{pmatrix}, h_{\tilde{3}} = \sigma h_3 = \begin{pmatrix} 2-y \\ x \end{pmatrix}.$$

Since $A_2 \cup A_3 = A_{\tilde{2}} \cup A_{\tilde{3}}$, the set $\{g, h_1, h_{\tilde{2}}, h_{\tilde{3}}, h_4, h_5\}$ gives another reptile system for the fractal A. Let $f_{\tilde{2}}$ and $f_{\tilde{3}}$ denote the new contractive maps in the corresponding IFS $\tilde{\mathcal{F}}$. It turns out that the neighbour maps for this IFS are different from the neighbour maps for $\mathcal{F}$. There are still 11 edge neighbours but the set of irrational rotations $\{a, a^-, b, b^-\}$ is replaced by a set of glide reflections $\{u, u^-, v, v^-\}$ (see Figure 5.11). Many of the arrows between vertices are also different. Figure 5.12 shows the sub-graph with vertices p, r, r^-.

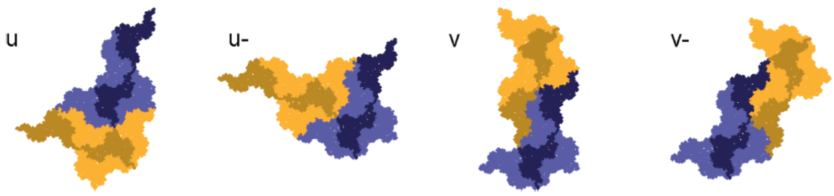

Figure 5.11: Second fractal pinwheel glide neighbours [BMT18]

There are 31 point neighbours, some of which are irrational rotations, meaning that the property of statistical circular symmetry is also exhibited here.

Together, the two fractal pinwheel tilings IFS satisfy the requirements of Definition 5.1 for a mixed tiling IFS $\hat{\mathcal{F}} = \{\mathcal{F}, \tilde{\mathcal{F}}\}$. Even though $f_i = f_{\tilde{i}}$ for $i = 1, 4, 5$

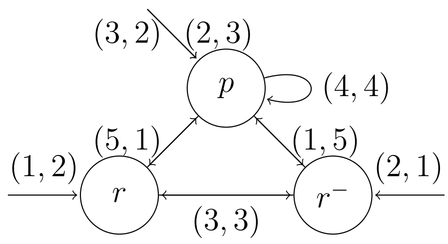

Figure 5.12: Second fractal pinwheel sub-neighbour graph

we still write $\tilde{1}, \tilde{4}, \tilde{5} \in [\tilde{5}]$ to explicitly denote that we are working in this IFS. Let $[N \cup \tilde{M}] := \{1, \cdots N, \tilde{1}, \cdots \tilde{M}\}$. From Definition 5.14, we know how to make tiling blowups $\hat{\Pi}(\theta)$ that are bounded for $\theta \in [5 \cup \tilde{5}]^k$ for any $k \in \mathbb{N}$ and unbounded for $\theta \in [5 \cup \tilde{5}]^\infty$.

Remark 5.23. It would be interesting to investigate the cohomology properties of mixed fractal pinwheel tiling spaces. As far as we can tell, no one has computed cohomology groups for a two-dimensional mixed tiling example. As mentioned above, the techniques of A & P or the extensions by G & M would not apply directly since the prototile set is not finite when considering the action of translation. There is an existing branch of tiling literature examining the action of different isometry groups on tiling cohomology (see [BDHS10] for example).

Remark 5.24. We end this section with a remark proposing a definition of neighbour maps and graphs in the mixed tiling setting, restricted to the case where the IFSs have one vertex. We believe all neighbour maps in this mixed setting are found by applying the interior automorphism $\Phi_{ij}(h) = f_{i_1}^{-1} h f_{j_1}$ for $(i, j) \in [N] \times [N] \cup [\tilde{N}] \times [\tilde{N}]$ starting with $h = id$. We construct a mixed neighbour graph, by setting the vertex set to be the set of proper neighbour maps generated by Φ_{ij} and letting $(k, l) \in [N] \times [N] \cup [\tilde{N}] \times [\tilde{N}]$ be a directed arrow from neighbours $\bar{h}$ to h if $\bar{h} = f_k^{-1} h f_l$. For the mixed fractal pinwheel example it is clear that there are at least 15 edge neighbours $\{p, r, r^-, s, s^-, t, t^-, a, a^-, b, b^-, u, u^-, v, v^-\}$ but it would be interesting to know whether there are any more.

5.4 Mixed Sierpinski

This section uses an example to show that the mixed tiling IFS theory also caters for tiling with fractal tiles that have no interiors. Recall the Sierpinski IFS $\mathcal{F} =$

$\{f_1, f_2, f_3\}$, with explicit maps defined in section 2.3.1. We define a second IFS $\tilde{\mathcal{F}}$ that includes the three maps from $\mathcal{F}$ plus the additional map

$$f_4 \begin{bmatrix} x \\ y \end{bmatrix} = \begin{bmatrix} \frac{1}{4} & 0 \\ 0 & \frac{1}{4} \end{bmatrix} \begin{bmatrix} x \\ y \end{bmatrix} + \begin{bmatrix} \frac{3}{4} \\ \frac{\sqrt{3}}{8}. \end{bmatrix}$$

We call this second IFS the 'Enhanced Sierpinski'. Figure 5.13 displays the attractor for the original Sierpinski and Enhanced Sierpinski side by side (denoted A and $\tilde{A}$ respectively). Together $\mathcal{F}$ and $\tilde{\mathcal{F}}$ satisfy the requirements of Definition 5.1 for a mixed tiling IFS. To construct bounded tilings $\hat{\Pi}(\tilde{1}1)$ and $\hat{\Pi}(1\tilde{1})$, we

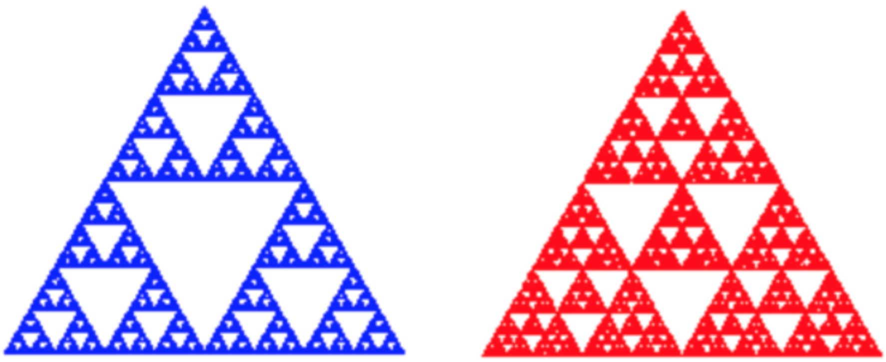

Figure 5.13: Sierpinski and Enhanced Sierpinski attractors

compute the sets $\Omega_{[1\tilde{1}]}$ and $\Omega_{[\tilde{1}1]}$ respectively:

$$\begin{aligned} \Omega_{[1\tilde{1}]} = \{ & 11\tilde{1}, 11\tilde{2}, 11\tilde{3}, 11\tilde{4}, 12\tilde{1}, 12\tilde{2}, 12\tilde{3}, 12\tilde{4}, \\ & 13\tilde{1}, 13\tilde{2}, 13\tilde{3}, 13\tilde{4}, 21\tilde{1}, 21\tilde{2}, 21\tilde{3}, 21\tilde{4}, \\ & 22\tilde{1}, 22\tilde{2}, 22\tilde{3}, 22\tilde{4}, 23\tilde{1}, 23\tilde{2}, 23\tilde{3}, 23\tilde{4}, \\ & 31\tilde{1}, 31\tilde{2}, 31\tilde{3}, 31\tilde{4}, 32\tilde{1}, 32\tilde{2}, 32\tilde{3}, 32\tilde{4}, \\ & 33\tilde{1}, 33\tilde{2}, 33\tilde{3}, 33\tilde{4}\}, \end{aligned}$$

$$\begin{aligned} \Omega_{[\tilde{1}1]} = \{ & \tilde{1}\tilde{1}1, \tilde{1}\tilde{1}2, \tilde{1}\tilde{1}3, \tilde{1}\tilde{2}1, \tilde{1}\tilde{2}2, \tilde{1}\tilde{2}3, \\ & \tilde{1}\tilde{3}1, \tilde{1}\tilde{3}2, \tilde{1}\tilde{3}3, \tilde{1}\tilde{4}, \tilde{2}\tilde{1}1, \tilde{2}\tilde{1}2, \tilde{2}\tilde{1}3, \\ & \tilde{2}\tilde{2}1, \tilde{2}\tilde{2}2, \tilde{2}\tilde{2}3, \tilde{2}\tilde{3}1, \tilde{2}\tilde{3}2, \tilde{2}\tilde{3}3, \tilde{2}\tilde{4}, \\ & \tilde{3}\tilde{1}1, \tilde{3}\tilde{1}2, \tilde{3}\tilde{1}3, \tilde{3}\tilde{2}1, \tilde{3}\tilde{2}2, \tilde{3}\tilde{2}3, \\ & \tilde{3}\tilde{3}1, \tilde{3}\tilde{3}2, \tilde{3}\tilde{3}3, \tilde{3}\tilde{4}, \tilde{4}1, \tilde{4}2, \tilde{4}3\}. \end{aligned}$$

Comparing Figures 5.14 and 5.15 we observe that some bounded tilings in the image of $\hat{\Pi}$ only contain tiles that are scaled copies of one IFS attractor while others contain scaled copies of both IFS attractors. Also, some bounded tiles are made from uniformly scaled tiles while others have tiles of multiple sizes. Figure 5.14 shows that all the tiles in $\hat{\Pi}(\tilde{1}1)$ are translations of the prototiles $s\tilde{A}$ and $s^2\tilde{A}$. In contrast, Figure 5.15 shows that all the tiles in $\hat{\Pi}(1\tilde{1})$ are translations of the prototiles sA and $s\tilde{A}$ (and thus all uniformly sized). The sets $\Omega_{[1\tilde{1}]}$ and $\Omega_{[\tilde{1}1]}$ have 36 and 33 members respectively. So, while $\hat{\Pi}(1\tilde{1})$ is made from 33 tiles $\hat{\Pi}(\tilde{1}1)$ is made from 36 tiles.

Remark 5.25. There is scope to investigate other mixed fractal tiling systems. Particularly, it would be interesting to find an example that satisfies an appropriately defined locally rigid condition. A variation on the rigid Williams IFS could be a candidate.

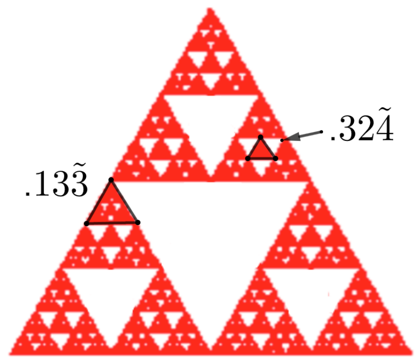

Figure 5.14: Mixed Sierpinski tiling $\hat{\Pi}(\tilde{1}1)$

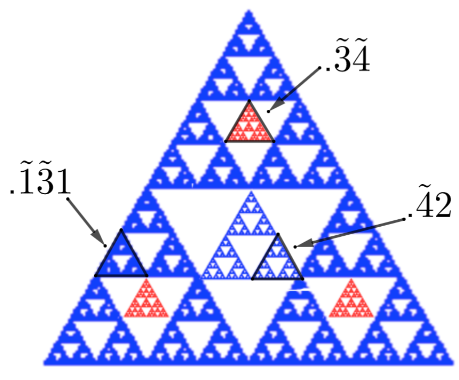

Figure 5.15: Mixed Sierpinski tiling $\hat{\Pi}(1\tilde{1})$

5.5 1-Variable Tiling IFS

Only at the very end of this thesis work did the connection between mixed tiling IFS and superfractal theory begin to be explored. We believe it is worth including a short section on this relation since it may be of interest to anyone familiar with either the tiling or superfractal theory. To introduce 1-variable IFS theory we follow the general notation and set-up in [Bar06].

Definition 5.26. A superIFS is a compact metric space $\mathbb{X}$ together with a collection of IFSs $\{\mathcal{F}_m : m = 1, 2 \cdots M\}$.

Let $\hat{\mathcal{F}} = \{\mathcal{F}_a, \mathcal{F}_b\}$ denote a superIFS with two member IFSs. For simplicity, we suppose that the graphs for both members have only one vertex. Let N_a and N_b denote the number of maps in $\mathcal{F}_a$ and $\mathcal{F}_b$ respectively. Let $[a, b]^\infty$ denote the strings of infinite length made from the letters a and b. The set $\hat{A}$, an element of $\mathbb{H}(\mathbb{H}(\mathbb{X}))$, denotes the attractor of $\hat{F}$. This attractor is the unique set given by

$$\hat{A} = \phi_{\hat{F}}([a, b]^\infty)$$

where $\phi_{\hat{F}} : [a, b]^\infty \to \mathbb{H}(\mathbb{X})$ is the code space mapping associated with $\hat{F}$. Elements of $\hat{A}$ are points $A_\theta \in \mathbb{H}(\mathbb{X})$ that can be expressed in the form

$$A_\theta = \phi_{\hat{F}}(\theta) = \lim_{k\to\infty} \mathcal{F}_{\theta_1} \circ \mathcal{F}_{\theta_2} \circ \cdots \mathcal{F}_{\theta_k}(\mathbb{X})$$

for $\theta \in [a, b]^\infty$. The set A_θ is called a 1-variable fractal set [Bar06].

To make the link to the tiling theory, we suppose that the IFSs in the superfractal satisfy the same conditions imposed for the mixed tiling IFS (recall Definition 5.1). All the maps in $\mathcal{F}_a$ and $\mathcal{F}_b$ have scaling powers that are integer powers of the same fixed $0 < s < 1$. Also, we assume that some attractor compatibility condition holds. A good example to keep in mind is the mixed Sierpinski from section 5.4. Using a 1-variable Sierpinski example follows a similar but greatly simplified approach to [FHH15] which studies the spectral asymptotics for general V-variable Sierpinski gaskets.

From superfractal theory, we know that each infinite string $\theta \in [a, b]^\infty$ has an associated 1-variable fractal set A_θ. For $\bar{a} \in [a, b]^\infty$, the 1-variable fractal set $A_{\bar{a}}$ is exactly the attractor of the IFS $\mathcal{F}_a$. For $\bar{ab} \in [a, b]^\infty$, the 1-variable fractal set $A_{\bar{ab}}$ is the attractor of the IFS $\mathcal{F}_a \circ \mathcal{F}_b$. The key idea is that each of these infinite strings corresponds to a whole space of tilings. In a similar style to the theory introduced in chapter 1, there is a natural address space, coding map, scaling sets and tiling map associated with each $\theta = [a, b]^\infty$. Suppose such a tiling map for some $\theta = [a, b]^\infty$ is denoted Π_θ. The idea is that bounded and unbounded tilings in the image of Π_θ are made from tiles that are scaled copies of the 1-variable fractal set A_θ. This is a major difference in comparison to the mixed tiling setting discussed at the beginning of this chapter. In that setting, all tilings are made from tiles that are scaled copies of $A_{\bar{a}}$ and $A_{\bar{b}}$. However, in the 1-variable IFS setting if we consider tilings associated with the string $\theta = \bar{ab}$ we observe that the tiles are all scaled copies of the set $A_{\bar{ab}}$ (the attractor of the IFS $\mathcal{F}_a \circ \mathcal{F}_b$). There is scope to explore further the intersection between the superfractal and tiling theory.

Bibliography

[AP98] J. E. Anderson, I. F. Putnam, Topological invariants for substitution tilings and their associated C*-algebras, *Ergod. Th. & Dynam. Sys.* 18 (1998) 509-537.

[Ban97] C. Bandt, Self-Similar Tilings and Patterns Described by Mappings, The mathematics of long-range aperiodic order (Waterloo, ON, 1995), *NATO Adv. Sci. Inst. Ser. C Math. Phys. Sci.*, vol. 489, Kluwer Acad. Publ., Dordrecht (1997) 45-83.

[Bar93] M. F. Barnsley, *Fractals everywhere*, 2nd ed., revised with the assistance of and with a foreword by Hawley Rising, III, Academic Press Professional, Boston, MA, 1993.

[Bar06] M. F. Barnsley, *Superfractals*, Cambridge University Press, Cambridge, 2006.

[BD08] M. Barge, B. Diamond, Cohomology in one-dimensional substitution tiling spaces, *Proc. Amer. Math. Soc.* 136(6) (2008) 2183-2191.

[BDHS10] M. Barge, B. Diamond, J. Hunton, L. Sadun, Cohomology of substitution tiling spaces, *Ergodic Theory Dynam. Systems*, 30(6) (2010) 1607-1627.

[BG92] C. Bandt, S. Graf, Self-similar sets VII. A characterization of self-similar fractals with positive Hausdorff measure. *Proc. Amer. Math. Soc.* 114 (1992) 995-1001.

[BHR05] C. Bandt, N. V. Hung, H. Rao, On the open set condition for self-similar fractals, *Proc. Amer. Math. Soc.* 134, no. 5 (2005) 1369-1374.

[BK10] H. Boulmezaoud, J. Kellendonk, Comparing different versions of tiling cohomology, *Topology Appl.* 157 (2010) 2225-2239.

[BM09] C. Bandt, M. Mesing, Self-affine fractals of finite type, Convex and fractal geometry, *Banach Center Publ., vol. 84, Polish Acad. Sci. Inst. Math.*,Warsaw (2009) 131-148.

[BM18] C. Bandt, D. Mekhontsev, New relatives of the Sierpinksi gasket, 2018. arXiv:1801.08325.

[BMT18] C. Bandt, D. Mekhontsev, A. Tetenov, A single fractal pinwheel tile, *Proc. Amer. Math. Soc.* 146 (2018), 1271-1285.

[BV14] M. F. Barnsley, A. Vince, Fractal tilings from iterated function systems, *Discrete and Computational Geometry,* 51 (2014) 729-752.

[BV17a] M. F. Barnsley, A. Vince, Self-similar polygonal tilings, *Amer. Math. Monthly,* 124:10 (2017) 905-921

[BV17b] M. F. Barnsley, A. Vince, Self-Similar Tilings of Fractal Blow-ups, 2017. arXiv:1709.09325v1.

[BV18] M. F. Barnsley, A. Vince, Tiling iterated function systems and Anderson-Putnam theory, 2018. arXiv:1805.00180.

[CR98] J. H. Conway, C. Radin, Quaquaversal tilings and rotations, *Invent. Math.* 132 no. 1 (1998) 179-188

[FHH15] U. Freiberg, B.M. Hambly, J.E Hutchinson, Spectral Asymptotics for V-Variable Sierpinksi Gaskets, 2015. arXiv:1502.00711v1.

[Fre08] D. Frettloh, Substitution tilings with statistical circular symmetry, *European J. Combin.* 29 no. 8 (2008) 1881-1893

[GM13] F. Gahler and G. R. Maloney, Cohomology of one-dimensional mixed substitution tiling spaces, *Topology Appl.* 160 (2013) 703-719.

[Hut81] J. Hutchinson, Fractals and self-similarity, *Indiana Univ. Math. J.* 30 (1981) 713-747.

[Man83] B. Mandelbrot, *The Fractal Geometry of Nature*, W. H. Freeman, New York, 1983.

[Mek] D. Mekhontsev, IFStile finder, https://ifstile.com.

[MW88] Mauldin, R.D. and Williams, S.C, Hausdorff dimension in graph directed constructions, *Trans. Amer. Math. Soc.*. 309 (1988) 811-829.

[Rad99] C. Radin, *Miles of tiles*, Student Mathematical Library, vol. 1, American Mathematical Society, Providence, RI, 1999.

[Rus16] D. Rust, Cohomology of Tiling Spaces: Beyond Primitive Substitutions, Ph.D dissertation, University of Leicester, 2016.

[RW92] C. Radin, M. Wolff. Space tilings and local isomorphism. *Geom. Ded.* 42 (1992) 355-360.

[Sad05] L. Sadun, Tiling, tiling spaces and topology, 2005. arXiv:math/0506054.

[Sad08] L. Sadun, *Topology of tiling spaces*, University Lecture Series, vol. 46, American Mathematical Society, Providence, RI, 2008.

[SW18] K. Steemson, C. Williams, Generalised Sierpinski Triangles, 2018. arXiv:1803.00411.

[ZHWD08] X. M. Zhang, R. Hitt, B.Wang and J. Ding, Sierpinski Pedal Triangles, *Fractals* 16(2) (2008) 141-150.